THE THREE-DIMENSIONAL STRUCTURE OF INTEGRINS AND THEIR LIGANDS, AND CONFORMATIONAL REGULATION OF CELL ADHESION

By TIMOTHY A. SPRINGER* AND JIA-HUAI WANG†

*CBR Institute for Biomedical Research, Department of Pathology, Harvard Medical School, Boston, Massachusetts 02115; †Dana-Farber Cancer Institute, Departments of Pediatrics, Biological Chemistry and Molecular Pharmacology, Harvard Medical School, Boston, Massachusetts 02115

Abstract

Integrins are a structurally elaborate family of adhesion molecules that transmit signals bidirectionally across the plasma membrane by undergoing large-scale structural rearrangements. By regulating cell-cell and cell-matrix contacts, integrins participate in a wide-range of biological interactions including development, tissue repair, angiogenesis, inflammation and hemostasis. From a therapeutic standpoint, integrins are probably the most important class of cell adhesion receptors. Structural investigations on integrin-ligand interactions reveal remarkable features in molecular detail. These details include the atomic basis for divalent cation-dependent ligand binding and how conformational signals are propagated long

0065-3233/04 $35.00

distances from one domain to another between the cytoplasm and the extracellular ligand binding site that regulate affinity for ligand, and conversely, cytosolic signaling pathways.

I. Introduction

Members of the integrin family of adhesion molecules are non-covalently associated α/β heterodimers that mediate cell-cell, cell-extracellular matrix, and cell-pathogen interactions by binding to distinct but often overlapping combinations of ligands. Eighteen different integrin α subunits and eight different β subunits are present in vertebrates, forming at least 24 $\alpha\beta$ heterodimers and perhaps making integrins the most structurally and functionally diverse family of cell adhesion molecules (Hynes, 1992; Springer, 1994) (Fig. 1). Half of integrin α subunits contain inserted (I) domains, which are the major ligand binding domains when present (Humphries, 2000; Shimaoka *et al.*, 2002). The structural and functional diversity and complexity of integrins allow this family of adhesion molecules to play pivotal roles in broad contexts of biology including inflammation, innate and antigen-specific immunity, hemostasis, wound healing, tissue morphogenesis, and regulation of cell growth and differentiation (Hynes, 1992; Springer, 1994). Conversely, dysregulation of integrins is involved in the pathogenesis of many disease states, from autoimmunity to thrombotic vascular diseases to cancer metastasis (Curley *et al.*, 1999). Therefore, extensive efforts to discover and develop integrin antagonists have been made for clinical applications.

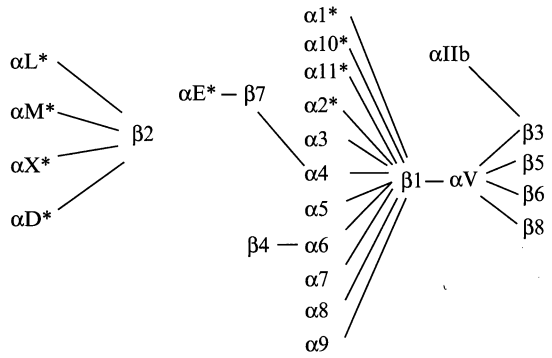

FIG. 1. Integrin α- and β-subunits form 24 heterodimers that recognize distinct but overlapping ligands. Half of the α subunits contain I domains (asterisks).

II. Conformational Regulation of Integrin Structure and Function

A. *Overall Picture of Integrin Heterodimers and Integrin Domains*

Integrins have a key role in organizing the cellular architecture of metazoan organisms. Furthermore, integrins are perhaps the only known family of adhesion molecules that can mediate migration of cells within tissues. Migration requires dynamic regulation both of integrin cytoplasmic domain association with cytoskeletal components, and extracellular domain binding to matrix components and cell surface glycoproteins. These functions are facilitated by the presence of two large, noncovalently associated subunits in integrins, each with a complex extracellular domain organization (Fig. 2). Each subunit spans the membrane, and the cytoplasmic domains with one exception (de Pereda *et al.*, 1999) are surprisingly short. Integrins are not found in prokaryotes, fungi, or plants but are present in the most primitive metazoans, including sponges and corals. By the time that *Drosophila* and *C. elegans* evolved, two of the main families of integrin α subunits were already present, which bind laminins and Arg-Gly-Asp (RGD)-containing matrix components (Hynes and Zhao, 2000). In the billion years of metazoan evolution, the number of extracellular domains and their organization in integrins has not changed, with the exception that in chordates, some integrin α subunits contain an inserted or I domain (Figs. 1 and 2).

The integrin α subunit ectodomain of >940 residues contains four domains (5 in I domain-containing integrins) and the β subunit of ~640 residues contains eight domains (Fig. 2). The crystal structure of the ectodomain of integrin $\alpha_v\beta_3$ revealed the structure, in a bent conformation, of eight of these domains, and a portion of a ninth (Fig. 2B) (Xiong *et al.*, 2001). The structures of integrin-EGF domains 2 and 3 of the β_2 subunit were determined by NMR, complementing a part of the missing portions of the $\alpha_v\beta_3$ structure (Beglova *et al.*, 2002). The N-terminal portions of the α and β subunits fold into the globular headpiece, which is connected through α and β tailpiece domains to the membrane (Du *et al.*, 1993; Takagi *et al.*, 2001; Weisel *et al.*, 1992; Xiong *et al.*, 2001). Dramatic rearrangements occur in the orientation of these domains during integrin activation (Fig. 3) (Takagi *et al.*, 2002). In this review we will focus primarily on the integrin headpiece, where ligands bind. However, it should be emphasized that in the bent conformation, extensive interfaces totaling over 4000 $Å^2$ of solvent accessible surface are buried between the headpiece and tailpiece and between the α tailpiece and β tailpiece. These interfaces stabilize the bent conformation, and are important in regulating

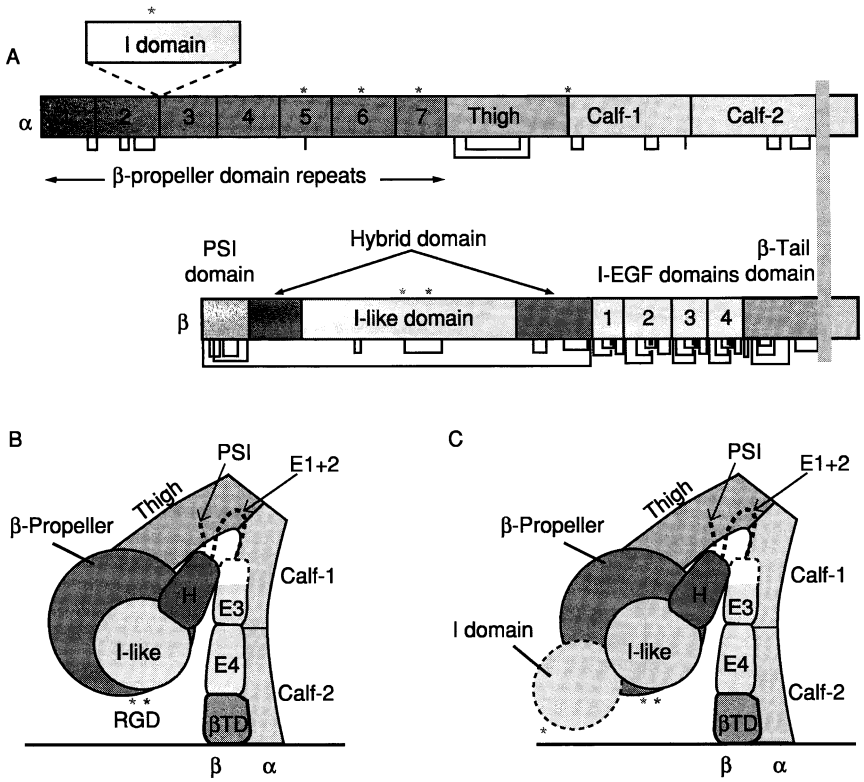

FIG. 2. Integrin architecture. (A) Organization of domains within the primary structure. Some α subunits contain an I domain inserted in the position denoted by the dotted lines. Cysteines and disulfide bonds are shown as lines below the stick figures. Red and blue asterisks denote Ca^{2+} and Mg^{2+} binding sites, respectively. (B) Arrangement of domains within the three-dimensional crystal structure of $\alpha_V\beta_3$ (Xiong *et al.*, 2001). Each domain is color coded as in A. (C) The structure in (B) with an I domain added. (See Color Insert.)

the equilibrium between the bent and extended integrin conformations (Fig. 3) (Luo *et al.*, 2003b; Takagi *et al.*, 2002).

B. vWF-Type A Domains: I Domain and I-Like Domain

All integrin β subunits and half of integrin α subunits contain von Willebrand factor-type A domains of about 200 amino acids, also referred to as the inserted (I) domain in the α-subunit and the I-like domain in the β subunit, respectively (Figs. 1, 2) (Humphries, 2000; Shimaoka *et al.*,

2002). Each domain adopts an α/β Rossmann fold with a metal ion dependent adhesion site (MIDAS) on the "top" of the domain, whereas its C and N-terminal connections are on the distal "bottom" face (Huang *et al.*, 2000; Lee *et al.*, 1995b; Shimaoka *et al.*, 2002; Xiong *et al.*, 2001) (Fig. 4A). Divalent cations are universally required for integrins to bind ligands and the metal at the MIDAS directly coordinates to a Glu or Asp residue in the ligand (Fig. 4B). This metal-dependent interaction through the MIDAS plays a central role in ligand recognition by the I and I-like domains.

C. *I Domain*

The I domain, which is inserted between blade 2 and 3 of the β-propeller domain of the α subunit (Fig. 2) (Springer, 1997), is a major ligand-binding domain and recognizes ligand directly when present (Diamond *et al.*, 1993; Michishita *et al.*, 1993). The ability of the I domain to bind ligand is controlled by conformational changes; the affinity of the I domain for its ligand is enhanced by downward axial displacement of its C-terminal α7-helix, which is conformationally linked to alterations of the MIDAS loops and Mg^{2+} coordination (Huth *et al.*, 2000; Shimaoka *et al.*, 2001, 2003b) (Fig. 4B, Fig. 5). In the case of $\alpha_L\beta_2$, compared to the default, low affinity conformation, downward displacements by one and two turns of α7-helix lead to intermediate- and high-affinity conformations with ~500 and 10,000-fold increased affinity, respectively (Shimaoka *et al.*, 2003b). A ratchet with a hydrophobic pocket stabilizes the β6-α7 loop in three alternative positions that correspond to downward movements of 0, 1, or 2 turns of 3_{10}-helix in the α7-helix (Fig. 5B, 5C). Disulfide bonds have been mutationally introduced that stabilize each of these three conformations and low, intermediate, and high affinity for ligand (Shimaoka *et al.*, 2003b) (Fig. 5A, 5C). Conversely, binding of ligand to the MIDAS of the I domain induces conformational change by stabilizing the high affinity conformation. This conformational change, which may be viewed as flowing from the ligand binding site to the α7-helix (Emsley *et al.*, 2000; Lee *et al.*, 1995b; Shimaoka *et al.*, 2003b) is identical to that flowing in reverse from the α7-helix to the ligand binding site (Shimaoka *et al.*, 2003b).

D. *I-Like Domain*

The β subunit I-like domain, which is inserted in the hybrid domain of the β-subunit (Fig. 2A), directly binds ligand in integrins that lack I domains in the α subunit (Fig. 3C, Fig. 6A). By contrast, when the I

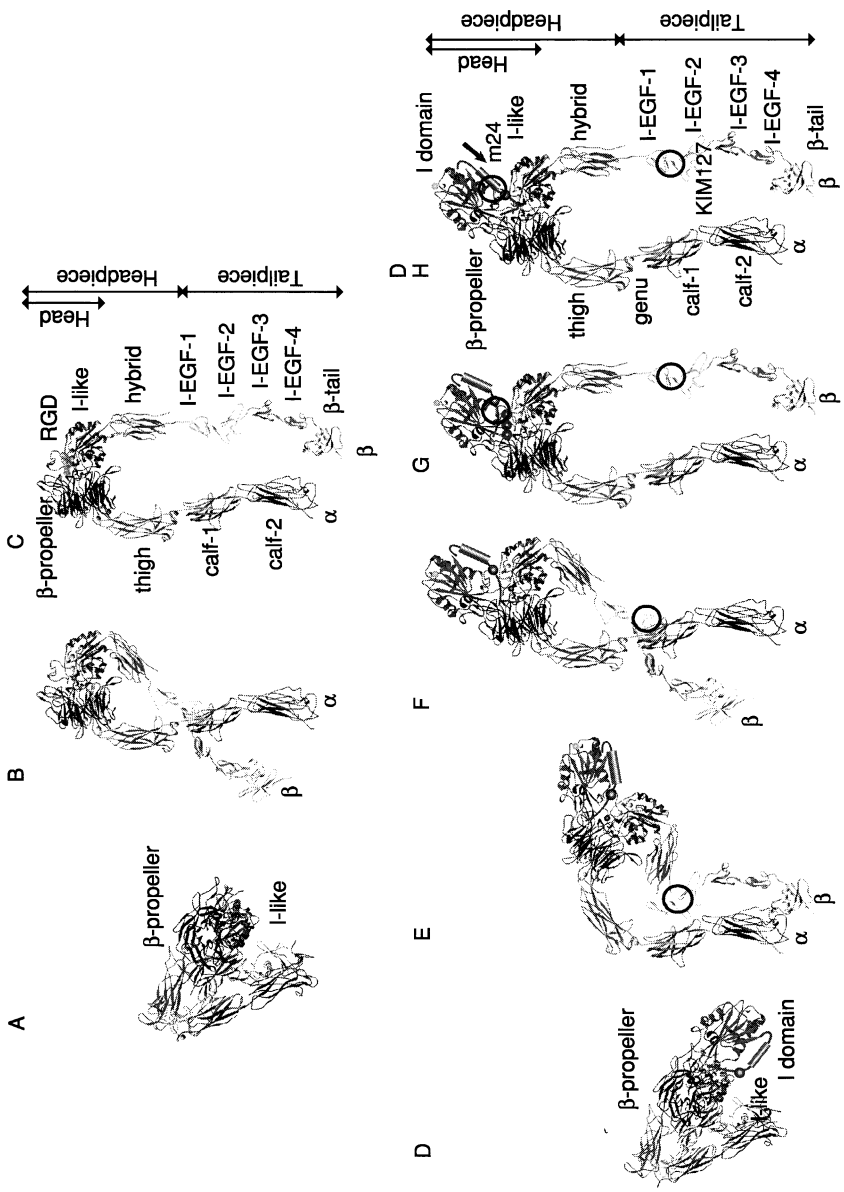
A
β-propeller
I-like
B
C
β-propeller
RGD
I-like
hybrid
I-EGF-1
I-EGF-2
I-EGF-3
I-EGF-4
β-tail
thigh
calf-1
calf-2
α
β
Head
Headpiece
Tailpiece
D
E
F
G
H
I domain
m24
genu
KIM127

domain is present the I-like domain functions indirectly by regulating the I domain (Fig. 3H, Fig. 6B). Compared to the I domain, the I-like domain contains two long loops, including one that is important for determining ligand specificity, and is referred to as the specificity-determining loop (SDL) (Takagi *et al.*, 1997). On either side of the MIDAS, the I-like domain contains two adjacent metal coordination sites, the ADMIDAS (*ad*jacent to *MIDAS*) and LIMBS (ligand-associated metal binding site) (Fig. 7A) (Xiong *et al.*, 2001, 2002).

The function of the I-like domain appears to be regulated by conformational changes similar to those observed in the I domain, in which a downward movement of the C-terminal α-helix allosterically alters the geometry of the MIDAS and increases the affinity for ligand (Shimaoka *et al.*, 2002; Takagi and Springer, 2002). Outward swing of the hybrid domain relative to the I-like domain (Figs. 3B, C and 6A) is thought to be coupled to the downward shift of the C-terminal α-helix of the I-like domain (Luo *et al.*, 2003b; Takagi *et al.*, 2002, 2003a).

E. β-Propeller Domain

The N-terminal region of the integrin α-subunit contains seven repeats of about 60 amino acids, which fold into a seven-bladed β-propeller domain (Springer, 1997; Xiong *et al.*, 2001) (Fig. 2A). A β-propeller domain with the same topology is also found in the trimeric G-protein β-subunit. The

---

FIG. 3. Conformational states for integrins. A–C. Model for $\alpha_V\beta_3$ integrin activation, with at least three conformations of the extracellular domain (Takagi *et al.*, 2002). (A) Bent, low affinity conformation. (B) Extended conformation with closed headpiece. (C) Extended conformation with open headpiece shown with bound RGD-mimetic peptide (green CPK). D–H. Model for $\alpha_L\beta_2$ integrin activation. (D) Bent conformation with low affinity. (E) and (F) $\alpha_L\beta_2$ with a closed headpiece and closed I domain in partially (E) or fully (F) extended states. (G) Extended conformation with open headpiece, and closed I domain, in the presence of α/β I-like allosteric antagonist, represented by three red spheres. (H) Extended conformation with open headpiece and open I domain. The models for all of the extracellular domains except for the I domain are based on conformational states of $\alpha_V\beta_3$ defined by negative stain electron microscopy (Takagi *et al.*, 2002), crystallography (Xiong *et al.*, 2002), NMR (Beglova *et al.*, 2002), and mapping of activation epitopes (Lu *et al.*, 2001a,c). The α_L I domain is a cartoon based on crystal structures (Shimaoka *et al.*, 2003b). The I domain is joined at the point of its insertion in the β-propeller domain but its orientation is arbitrary; it is shown at slightly larger scale for emphasis. The C-terminal I domain α-helix is represented by a red cylinder, and α_L Glu-310 in the linker as a blue sphere. The positions of activation epitopes m24 and KIM127 are circled only in the conformations in which they are thought to be exposed. (See Color Insert.)

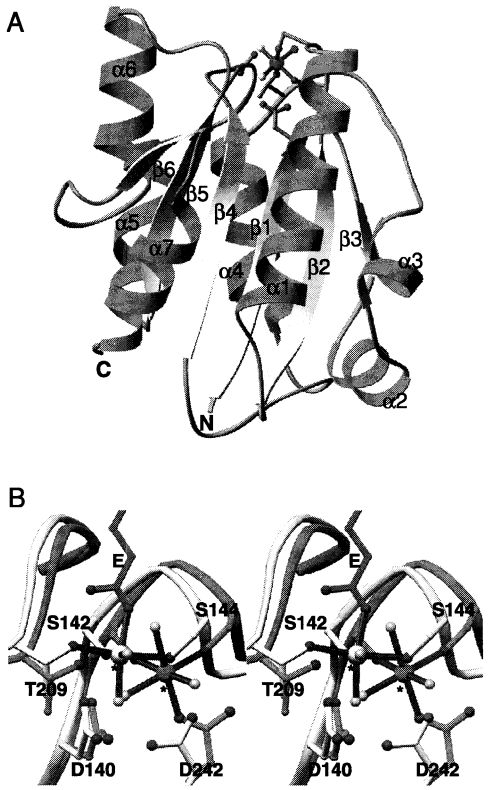

FIG. 4. α I domain structure and MIDAS conformational change. (A) Ribbon diagram of the α_M I domain in the open conformation (Lee *et al.*, 1995b). The β-strands (yellow), α-helices (cyan), and the N and C termini are labeled. The Mg ion is shown as a green sphere, and primary coordination bonds are blue. Side chains of residues that form primary or secondary coordinations to the metal ion are shown with grey bonds and carbon atoms and red oxygen atoms, and the oxygen of the ligand-mimetic Glu from another I domain is magenta. Coordinating water molecule oxygens are gold. Prepared with Ribbons (Carson, 1997). (B) Stereo view of alternative conformations of the α_M MIDAS. The backbone, coordinating side chain bonds, and metals (labeled with asterisks) are shown in yellow (open conformation) and cyan (closed conformation). The coordinating glutamate residue from the ligand-mimetic neighboring α_M I domain in α_M is in magenta. Primary coordination bonds to the metals are in blue. Oxygen atoms of the coordinating side chains and water molecules are red and gold, respectively. The 1IDO open α_M structure (Lee *et al.*, 1995a) was superimposed on the closed 1JLM α_M structure (Lee *et al.*, 1995b) using residues 132–141, 166–206, 211–241, 246–270, and 287–294. (See Color Insert.)

β-propeller domain directly participates in ligand recognition in those integrins that lack α I domains (Humphries, 2000).

F. Structure of the Headpiece in Integrins that Lack I Domains

The structure of $\alpha_v\beta_3$ reveals that the I-like domain makes extensive contact with the β-propeller domain, with the "top," ligand-binding faces of each domain oriented at about 90° to one another (Fig. 3A, B) (Xiong *et al.*, 2001). Loops in blades 2, 3, and 4 of the β-propeller domain are prominent in the ligand binding site. The structure of $\alpha_v\beta_3$ in complex with a cyclic peptide containing an Arg-Gly-Asp (RGD) sequence demonstrated binding to both the α and β subunits at the interface between the β-propeller and I-like domains (Fig. 3C). The Asp carboxylic acid side chain coordinates directly to the metal of the β subunit I-like domain MIDAS (Fig. 7A), while the Arg side chain binds to the α subunit β-propeller domain (Xiong *et al.*, 2002). Mapping by mutagenesis of residues important in binding to fibrinogen, the biological ligand of $\alpha_{IIb}\beta_3$, demonstrates a much larger interaction surface, centered on blades 2 to 4 of the α subunit β-propeller domain and the SDL loop of the β subunit I-like domain (Kamata *et al.*, 2001; Puzon-McLaughlin *et al.*, 2000).

Intriguing structural homology exists between the integrin β-propeller domain and the trimeric G protein β subunit, and between integrin I and I-like domains and G protein α subunits (Springer, 1997; Xiong *et al.*, 2001). Dissociation of these domains upon activation occurs in G proteins; however, in integrin activation there is little rigid body movement of the β-propeller domain relative to the I-like domain (Luo *et al.*, 2003a). Instead, ligand-binding affinity appears to be regulated primarily by conformational changes in loops of the I-like domain and possibly also in the β-propeller domain.

G. Signal Transmission Across the Plasma Membrane

Intracellular signaling pathways that are activated by other receptors (e.g., receptors coupled to G proteins or tyrosine kinases) impinge on integrin cytoplasmic domains and enhance the affinity of the extracellular headpiece for ligand. Recently the basis for bidirectional signal transmission across the membrane by integrins has been explained. The integrin α and β cytoplasmic tails associate with each other and constrain the integrin in its inactive form. Dissociation of the $\alpha\beta$ cytoplasmic tails by signals within the cell leads to the activation of the extracellular parts of the integrin (Kim *et al.*, 2003; Lu *et al.*, 2001d; Takagi *et al.*, 2001, 2002;

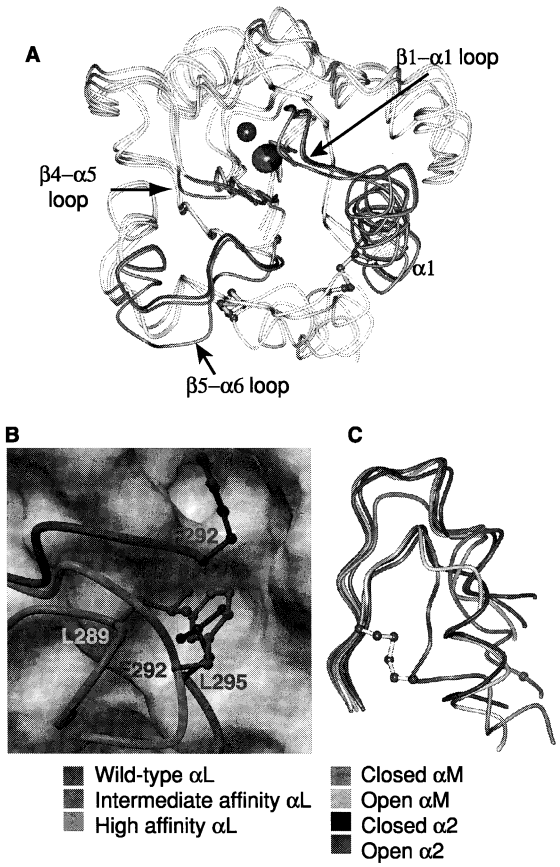

FIG. 5. Propagation of conformational change in the I domain. (A) The structures of the unliganded wild type, intermediate affinity, and high affinity αL I domains (Shimaoka *et al.*, 2003b). The three unliganded αL I domain backbones are shown superimposed and viewed centered on the MIDAS. Regions of the backbones that differ structurally are labeled and color keyed; other backbone regions are grey. The metal ions at the MIDAS and the atoms in the mutationally introduced, disulfide linked cysteine atoms are shown in the same colors as the backbone regions that differ; the cysteine sidechain bonds are yellow. The position of the missing metal ion in the high affinity structure is simulated with a smaller sphere. β6-α7 loop and α7 are shown in grey for clarity; differences in these regions are shown in (B) and (C). (B) The hydrophobic pocket that acts as a detent for the rachet-like movement of the β6-α7 loop. The backbone of the β6-α7 loop and the three residues that occupy the same hydrophobic pocket in the three different conformational states are color keyed. The pocket is shown as a GRASP van der Waals surface using the wild-type 1LFA structure with the residues from 287 to the C-terminus deleted. The upper hydrophobic pocket is also shown, which is occupied only in the closed conformation (by F292 which is shown in the wild type structure along with L295). For the closed conformation the β6-α7

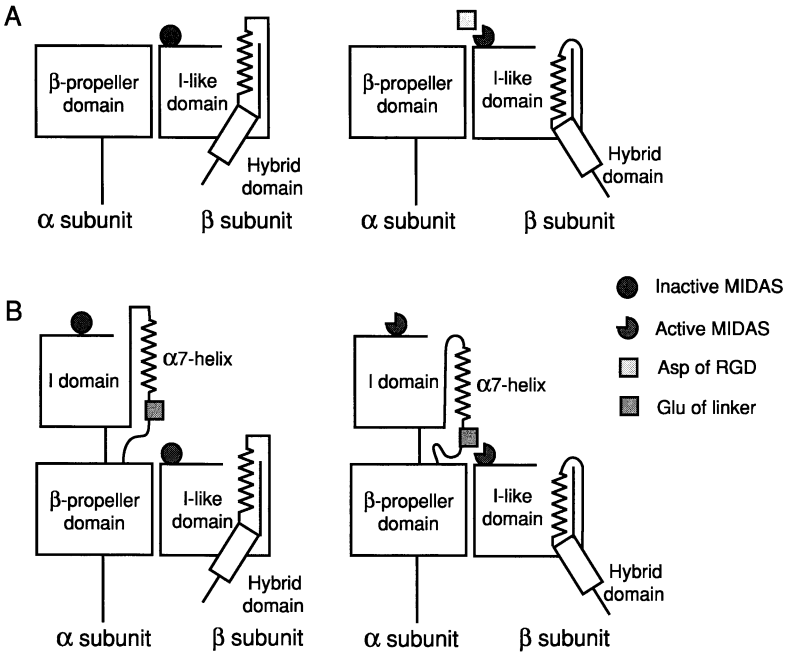

FIG. 6. Schematic drawing of conformational change in α I and β I-like domains and its coupling. (A) Integrins that lack α I domains. Swing-out of the hybrid domain is depicted as demonstrated for $\alpha_v\beta_3$ and $\alpha_5\beta_1$ (Takagi *et al.*, 2002, 2003a). Activation of the I-like domain is coupled to β I-like α7-helix downward displacement in both integrins that contain and lack α I domains (Luo *et al.*, 2004b; Yang *et al.*, 2004a), providing a mechanism for coupling activation to hybrid domain swing-out (Takagi *et al.*, 2002, 2003a). (B) In integrins that contain I domains, an invariant Glu in the linker following the α I α7-helix functions as an intrinsic ligand. Its binding to the β I-like MIDAS activates the α I MIDAS (Yang *et al.*, 2004b).

Vinogradova *et al.*, 2002). NMR studies reveal a weak association between the integrin α_{IIb} and β_3 subunit cytoplasmic domains, and that this association is disrupted by mutations that are known to activate integrins, and by binding of the β subunit cytoplasmic domain to the cytoskeletal

mainchain trace is broken between F292 and L295 for clarity. On the otherwise grey GRASP surface, hydrophobic residues are colored yellow. (C) The C-terminal fragments encompassing the β6-α7 loop for the three unligated α_L conformations and open and closed α_2 and α_M I domain structures (see color keys). The sidechain bonds of Cys-287 and Cys-294 in the designed disulfide bridge in the high affinity mutant are shown in yellow; the Cα atom of Cys-299 in the designed disulfide of the intermediate mutant is shown as a green sphere. (See Color Insert.)

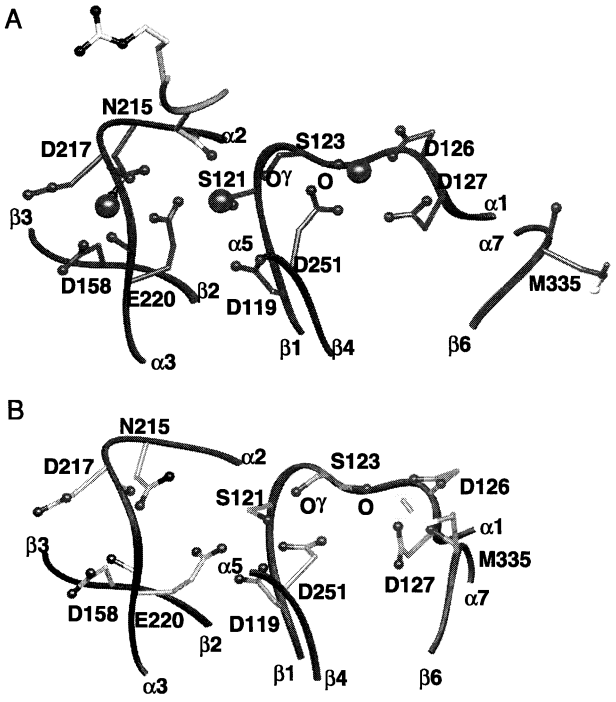

FIG. 7. The linear cluster of metal binding sites in the β I-like domain. (A) The liganded $\alpha_v\beta_3$ structure in Mn^{2+} with RGD (Xiong *et al.*, 2002) in gold. (B) The unliganded $\alpha_v\beta_3$ structure in Ca^{2+} (Xiong *et al.*, 2001). The structures were superimposed by using the I-like domain, so that equivalent positions in (A) and (B) are vertically aligned. The orientation is with the LIMBS, MIDAS, and ADMIDAS from left to right. Mn^{2+} and Ca^{2+} ions are large magenta and yellow spheres, respectively. All putative metal coordinating sidechains and backbone carbonyl groups are shown, with N, O, and S atoms in blue, red, and yellow, respectively. The carbonyl and sidechain oxygens of S123 are marked O and Oγ, respectively. (See Color Insert.)

protein talin, another known integrin activator (Garcia-Alvarez *et al.*, 2003; Vinogradova *et al.*, 2002; Weljie *et al.*, 2002). Fluorescence resonance energy transfer studies on $\alpha_L\beta_2$ demonstrate that the cytoplasmic domains separate upon activation of signaling pathways or talin activation within the cell, and upon binding of ligand to the extracellular domain (Kim *et al.*, 2003). Peptides containing integrin α and β subunit transmembrane domains form homodimers and homotrimers in detergent micelles (Li *et al.*, 2001, 2003); however, the physiologically relevant heterodimers fail to form under the same conditions, and homomeric interactions have not been demonstrated in lipid bilayers. Fluorescence resonance energy

transfer (FRET) studies demonstrate that activation of $\alpha_L\beta_2$ does not lead to homomeric association (Kim *et al.*, 2004). Cysteine scanning and disulfide bond formation between the α_{IIb} and β_3 transmembrane domains demonstrates a specific α-helical interface between them in the resting state, and that the α_{IIb} and β_3 transmembrane domains separate after activation (Luo *et al.*, 2004a). Again in this system, heterodimer separation does not lead to homomeric interactions.

H. Overall Conformational Change in the Ectodomain

In the latent, low-affinity state, the integrin assumes a bent conformation (Fig. 3A) (Beglova *et al.*, 2002; Takagi *et al.*, 2002). The C-terminal residues in the α_v and β_3 subunits in the bent crystal structure are close together (Xiong *et al.*, 2001), and only a few residues thereafter the transmembrane domains begin. Therefore, separation of the transmembrane domains would destabilize the interface between the α subunit calf-1 and calf-2 leg domains and the β subunit I-EGF3, I-EGF4, and β-tail leg domains (Fig. 3). Destabilizing the interface between the α and β legs in the tailpiece would in turn destabilize the tailpiece-headpiece interface, and induce a switchblade-like opening to an extended conformation (Fig. 3). This extension re-orients the ligand binding face and exposes activation epitopes in the tailpiece. In the extended conformation, two different conformations of the headpiece, termed closed (Fig. 3B) and open (Fig. 3C), are seen (Takagi *et al.*, 2002). In the bent conformation only the closed conformation of the headpiece is present (Xiong *et al.*, 2001). Therefore, extension facilitates adoption of the open conformation of the headpiece, which corresponds to the ligand-bound and high affinity conformation (Takagi *et al.*, 2002, 2003a). Between the closed and open headpiece conformations, there is a marked change in orientation between the I-like domain and hybrid domain (Fig. 3B, C). Electron microscopic studies on both $\alpha_{IIb}\beta_3$ and $\alpha_5\beta_1$ directly demonstrate that binding induces the open headpiece with the swung-out hybrid domain (Takagi *et al.*, 2002, 2003a), and swing-out is also supported by solution X-ray scattering studies on ligand-bound $\alpha_5\beta_1$ (Mould *et al.*, 2003c) and exposure of epitopes on the hybrid domain (Mould *et al.*, 2003b). Notably, many antibody epitopes that are buried in the bent conformation become exposed in the extended conformation (Beglova *et al.*, 2002).

In solution and apparently on the cell surface as well, integrins are not fixed in a particular conformation, but equilibrate between them (Takagi *et al.*, 2002) (Fig. 3A–C). Whether the equilibrium favors the bent, low affinity conformation or the extended, high affinity conformation is affected by the presence of activating intracellular factors and the

concentration of extracellular ligands. Activation by signals within the cell induces straightening and stabilizes the extended form. Binding of extracellular ligands also stabilizes the extended conformation and therefore enhances the separation of integrin tails, which transmits signals to the cytoplasm. Therefore, transition from the bent to the extended conformation is a bi-directional, allosteric mechanism for relaying conformational signals between the integrin headpiece and the cytoplasmic domains. All biological integrin ligands are multivalent, and therefore can also induce integrin clustering, which appears to be required, in addition to conformational change, for outside-in signaling.

I. Bistability of the β I-Like Domain

As described previously, EM studies show two distinct orientations between the I-like and hybrid domains. Ligand binding induces hybrid domain swing-out in solution as revealed by EM and apparently on cell surfaces as revealed by activation and "ligand-induced binding site" epitope exposure (Beglova *et al.*, 2002; Mould *et al.*, 2003b; Takagi *et al.*, 2002, 2003a). Consistent with these observations, it was suggested that downward movement of the β I-like α7-helix, analogous to that seen in α I domains, couples ligand binding affinity to hybrid domain swing-out (Takagi *et al.*, 2002). An N-glycosylation site introduced into the acute angle between the I-like and hybrid domains, designed to act as a wedge and stabilize the more obtuse angle in the open headpiece, activates ligand binding and integrin extension as predicted (Luo *et al.*, 2003b). An activating mutation in the β_1 I-like α7-helix supports the notion that this is an allosterically important region (Mould *et al.*, 2003b) and an activation epitope maps to the neighboring α1-helix (Mould *et al.*, 2002).

Two recent mutational studies provide direct evidence that downward movement of the α7-helix of the β I-like domain activates ligand binding. Mutagenic introduction of a disulfide bond between the β I-like β6-strand and α7-helix designed to stabilize the α7-helix in the conformation seen in the bent crystal structure abolished the ability to activate ligand binding by integrin $\alpha_{IIb}\beta_3$. By contrast, introduction of a disulfide bond into the β6-α7 loop that was designed to induce downward α7-helix displacement constitutively activated ligand binding (Luo *et al.*, 2004b). In another study, the effect of α7-helix displacement on the β6-α7 loop was mimicked by shortening the α7-helix by 4 residue deletions of $\sim$1 turn of α7-helix. Two independent 4-residue deletions were tested in the β_2 and β_7 subunits. The $\alpha_L\beta_2$ mutants exhibit constitutive high affinity for ICAM-1, and full exposure of an activation epitope in the β_2 I-like domain. The $\alpha_4\beta_7$ mutants show the active phenotype of firm adhesion, rather than rolling

adhesion, on the ligand mucosal addressin cell adhesion molecule-1 (MAdCAM-1) in a parallel plate flow chamber (Yang *et al.*, 2004a).

In the linear cluster of three metal ion binding sites in the β I-like domain (Fig. 7), the two outer sites regulate ligand binding by the middle MIDAS site (Chen *et al.*, 2003). These sites were mutated in the integrin $\alpha_4\beta_7$, and the effect studied on rolling adhesion on MAdCAM-1 substrates, which is hypothesized to be mediated by the extended conformation with the closed headpiece, with low or intermediate affinity, and firm adhesion on MAdCAM-1 substrates, which is hypothesized to be mediated by the extended conformation with the open headpiece, with high affinity (Chen *et al.*, 2003). Wild-type $\alpha_4\beta_7$ mediates rolling adhesion in Ca^{2+} and in contrast, firm adhesion in Mg^{2+} or Mn^{2+}. The middle MIDAS site is required for both rolling and firm adhesion. One polar site, the ADMIDAS, is required for rolling, because its mutation results in firm adhesion, no matter what divalent cation is present. The other polar site, the LIMBS, is required for firm adhesion, because its mutation results in rolling, no matter the divalent cation. The LIMBS mediates the positive regulatory effects of low Ca^{2+} concentrations, which synergize with Mg^{2+}, whereas the ADMIDAS mediates the negative regulatory effects of higher Ca^{2+} concentrations, which are competed by Mn^{2+}. The bipolar sites thus stabilize two alternative phases of adhesion. The higher affinity of Ca^{2+} than Mg^{2+} at the LIMBS is explained by the presence of three carbonyl O coordinations, for which Ca^{2+} has greater propensity than Mg^{2+} (Fig. 7A). The activating effect of Mn^{2+} and inhibitory effect of Ca^{2+} at the ADMIDAS may similarly be explained by the propensity of Ca^{2+} but not Mn^{2+} to form a carbonyl O coordination to the backbone of the $\beta6$-$\alpha7$ loop (Fig. 7B). This carbonyl coordination to Ca^{2+} seen in closed structures with Ca^{2+} (Fig. 7B) but with Mn^{2+} or Mn^{2+} plus ligand (Fig. 7A) (Xiong *et al.*, 2002) stabilizes the $\beta6$-$\alpha7$ loop against downward displacement with the $\alpha7$-helix in the postulated high affinity state of the β I-like domain. The ADMIDAS in some integrins appears required for downward movement of the $\alpha7$-helix, because in $\alpha_5\beta_1$ mutation of this site inhibits activation epitope exposure and ligand binding (Mould *et al.*, 2003a); this effect was not seen with $\alpha_4\beta_7$.

J. Activation of Integrins that Contain I Domains

In integrins that contain I domains, the I domain binds ligand, whereas the β-propeller and I-like domains have a regulatory role (Fig. 3D–H and Fig. 6B) (Lu *et al.*, 2001b,c). The bottom of the I domain is connected at its N- and C-termini to blades 2 and 3 of the β-propeller, respectively (Figs. 2A, 4A). A linker of ~15 residues C-terminal to the I domain must therefore

locate near the β-propeller/I-like domain interface, i.e., to the ligand-binding face in integrins that lack I domains. This linker contains an invariant Glu residue, and its mutation abolishes ligand binding by both $\alpha_L\beta_2$ and $\alpha_M\beta_2$ (Alonso *et al.*, 2002; Huth *et al.*, 2000). It has been proposed that this universally conserved Glu residue is an "intrinsic ligand," and that binding of the activated β_2 I-like domain to this intrinsic ligand pulls the C-terminal α7-helix of the α I domain downward, and activates high affinity for ligand (Fig. 6B) (Alonso *et al.*, 2002; Shimaoka *et al.*, 2002; Takagi and Springer, 2002). Indeed, recent experiments demonstrate signal transmission between the α I linker and β I-like MIDAS by a receptor-like interaction (Yang *et al.*, 2004b). Second-site reversion with complementing Cys mutations was used to demonstrate the interaction. Mutation of the invariant Glu in the linker, α_L-Glu-310, to Cys or Ala, abolished ligand binding by $\alpha_L\beta_2$. Similarly, mutation of either of two non-metal-coordinating residues that flank the Mg^{2+} of the β_2 I-like MIDAS, β_2-Ala-210 or β_2-Tyr-115, to Cys also abolished ligand binding. By contrast, the double mutation of α_L-E310C with either β_2-A210C or β_2-Y115C forms a disulfide bond that constitutively activates ligand binding. Thus, the α7 helix and its linker function as a pull spring. The results suggest that in integrins that contain I domains, the Glu in the linker functions as an intrinsic ligand for the β I-like domain, and that when these integrins are activated, the β I-like MIDAS binds to the Glu, pulls the spring, and thereby activates the α I domain.

K. Integrin Antagonists

Three antagonists to integrin $\alpha_{IIb}\beta_3$, the platelet receptor for fibrinogen, have been approved by the FDA for acute treatment and prevention of thrombosis. These are an antibody Fab fragment, and two small molecule RGD mimetics, all of which competitively antagonize fibrinogen binding (Scarborough and Gretler, 2000). An antibody to the α I domain of $\alpha_L\beta_2$ which competitively blocks binding to ICAM-1 was recently approved for therapy of mild to severe plaque psoriasis, an autoimmune disease (Gordon *et al.*, 2003). Small molecule antagonists are also under development to $\alpha_v\beta_3$ and $\alpha_v\beta_5$ for blocking tumor metastasis, angiogenesis and bone resorption (Varner and Cheresh, 1996), and to β_2 integrins and α_4 integrins on leukocytes for treating autoimmune diseases and other inflammatory disorders (Giblin and Kelly, 2001; Yusuf-Makagiansar *et al.*, 2002).

Small molecule antagonists have been used to obtain important insights into the conformational regulation of integrin structure and function (Shimaoka and Springer, 2003). The ability of ligands and ligand-mimetic

antagonists to induce conformational change in integrins has important clinical implications. $\alpha_{IIb}\beta_3$ antagonists expose LIBS epitopes on the surface of circulating platelets in treated patients. A small subset of patients have pre-existing LIBS antibodies, which cause thrombocytopenia after treatment (Billheimer *et al.*, 2002; Scarborough and Gretler, 2000). The current $\alpha_{IIb}\beta_3$ antagonists are designed for acute indications and have short *in vivo* half-lives. After drug dissociates from $\alpha_{IIb}\beta_3$ on live platelets, $\alpha_{IIb}\beta_3$ rapidly loses LIBS epitopes, and thus returns to the bent, low-affinity conformation (Kouns *et al.*, 1992). By contrast, if antagonist-treated platelets are fixed, and then antagonist is washed out, $\alpha_{IIb}\beta_3$ retains LIBS epitopes and has high affinity for fibrinogen (Du *et al.*, 1991). It is most important therapeutically that the antagonist-induced, high affinity conformation of $\alpha_{IIb}\beta_3$ is rapidly reversible *in vivo*; otherwise, antagonist dissociation and clearance would trigger thrombosis.

Two distinct classes of integrin antagonists have been discovered for the integrin $\alpha_L\beta_2$. In contrast to the competitive antagonists described previously, each acts allosterically (Shimaoka and Springer, 2003). α I allosteric antagonists bind between the α7-helix and the body of the I domain, and stabilize the domain in the closed, low affinity conformation (Kallen *et al.*, 1999) (Fig. 8). Mutant $\alpha_L\beta_2$ with the I domain locked in the high affinity, open conformation with a disulfide bond is completely resistant to inhibition (Lu *et al.*, 2001b). As assayed by epitope exposure, the conformation of the α_L I domain is coupled to the overall bent/extended integrin conformation through residue α_L-Glu-310 in the I domain linker; α I allosteric antagonists stabilize the bent conformation (Salas *et al.*, 2002, 2004; Shimaoka *et al.*, 2003a; Woska *et al.*, 2001).

α/β I-like allosteric antagonists appear to bind to a site in I domain-containing integrins (Fig. 3G) very similar to the site to which RGD-mimetics bind in integrins that lack I domains (Fig. 3C) (Shimaoka *et al.*, 2003a). These antagonists require the β_2 I-like MIDAS but not the α I domain for binding. Integrins that are stabilized in high affinity states either by disulfides within the α I domain, or by disulfides between the α I domain linker and residues adjacent to the β I-like MIDAS, are resistant to inhibition (Lu *et al.*, 2001b; Shimaoka *et al.*, 2003a; Yang *et al.*, 2004b). α/β I-like allosteric antagonists, like RGD-mimetic competitive antagonists, induce integrin extension as assayed by epitope exposure. However, they uncouple extension from I domain activation, revealing their binding site at the β I-like MIDAS to be a critical site for relaying conformational signals within I domain-containing integrins (Fig. 3G).

β_2 integrins primarily function in firm adhesion; they also can contribute to rolling adhesion, although markedly less well than α_4 integrins or selectins. Activated wild-type $\alpha_L\beta_2$, mutant high affinity $\alpha_L\beta_2$, and mutant

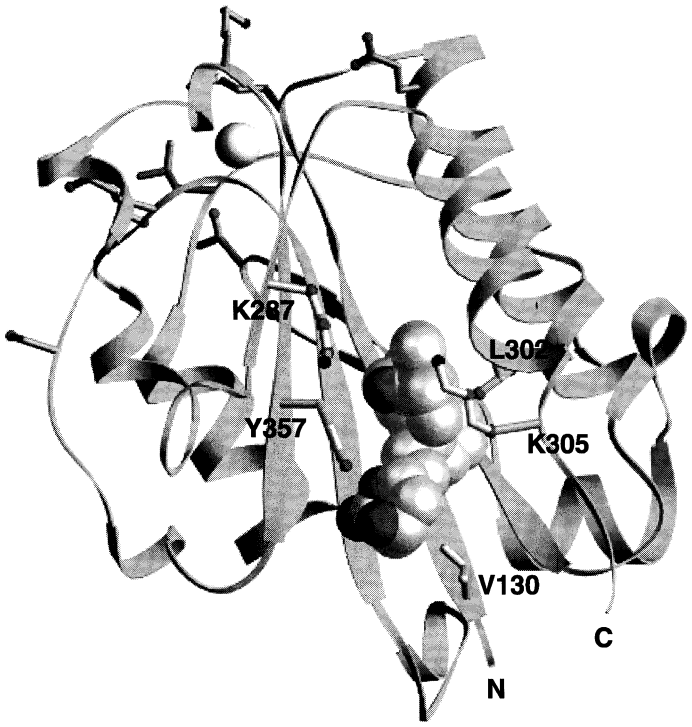

FIG. 8. Ribbon diagram of the α_L I domain in complex with an α I allosteric antagonist (Kallen *et al.*, 1999). The α I allosteric antagonist (shown by CPK with silver carbon atoms and red oxygen atoms) binds in the hydrophobic pocket underneath the C-terminal α-helix and stabilizes the I domain in the closed conformation. The side chains within the antagonist-binding pocket are shown with gold bonds and carbon atoms, red oxygen atoms, and blue nitrogen atoms. The residues critical for binding to ICAM-1 and ICAM-2 are shown with purple side chains and yellow sulfur, red oxygen, and blue nitrogen atoms. Note that these residues are located around the MIDAS, distal from the antagonist binding site. (See Color Insert.)

high affinity isolated, surface-expressed α_L I domains mediate firm adhesion. By contrast, resting, wild type $\alpha_L\beta_2$ and isolated surface-expressed wild type I domains mediate rolling adhesion (Salas *et al.*, 2002). α/β I-like allosteric antagonists inhibit firm adhesion, but because they induce the extended integrin conformation, they actually enhance rolling adhesion through $\alpha_L\beta_2$ (Salas *et al.*, 2004). This remarkable effect is seen both *in vitro* and *in vivo*.

III. Integrin/Ligand Interactions

The integrin counter-receptors on the cell surface include some members of immunoglobulin superfamily (IgSF) and the cadherin family. Ligands in ECM include collagen, laminin, fibronectin, fibrinogen, vitronectin, thrombospondin, and osteopontin. Structural investigations on integrin/ligand interactions have revealed intriguing features of these interactions with molecular detail. Figure 9 shows the integrin-binding domain structures of some representative ligands.

A. IgSF Protein as Counter-Receptor

Many of IgSF members are important cell adhesion molecules. What we will be discussing here is a subset of the IgSF proteins that share a greater sequence homology within the subset than to the other IgSF members and serve as counter-receptors for integrins. These are the intercellular adhesion molecules (ICAMs, including ICAM-1, ICAM-2, ICAM-3, ICAM-4 and ICAM-5, etc.), vascular adhesion molecule-1 (VCAM-1), and mucosal addressin cell adhesion molecule-1 (MAdCAM-1). As transmembrane glycoproteins, they are known to be composed of 2–9 IgSF domains in tandem

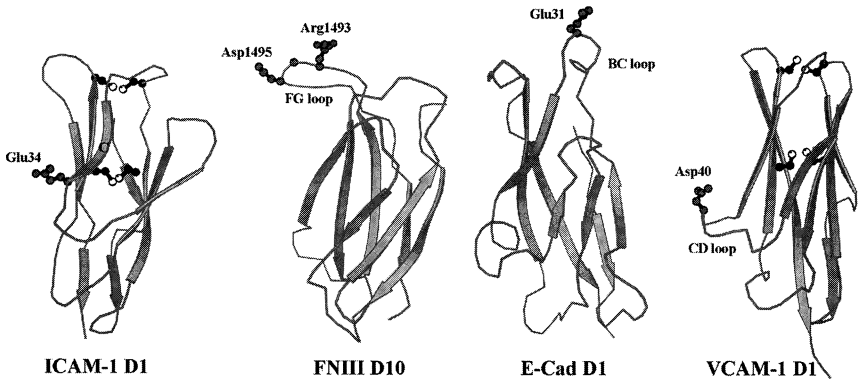

FIG. 9. Ribbon diagram of integrin-binding domain structures of four representative integrin ligands: ICAM-1 domain 1 (ICAM-1 D1), 10th fibronectin type III repeat (FNIII D10), E-cadherin domain 1 (E-Cad D1), and VCAM-1 domain 1 (VCAM-1 D1). In the figure, those key integrin-binding acidic residues are shown in red ball-and-stick model. They are located at the end of the C strand of IgSF domain (ICAM-1 D1), at the tip of the FG loop of FNIII domain (FNIII D10), at the tip of the BC loop of cadherin domain (E-Cad D1), and at the tip of the CD loop of IgSF domain (VCAM-1 D1), respectively. The figure demonstrates the diversity of integrin-binding modes to structurally very similar domains. The figure was prepared with MOLSCRIPT. (See Color Insert.)

on cell surface. The crystal structures of biologically the most important N-terminal two-domain fragment of ICAM-1 (Fig. 9), ICAM-2, VCAM-1 (Fig. 9) and MAdCAM-1 are known and reviewed (Wang and Springer, 1998). Here we offer a brief summary on the structural features of these molecules in the context of being integrin counter-receptors and then discuss most recent progress in structural studies on ICAM-1/α_L β_2 interactions.

1. Both domain 1 and 2 (D1 and D2) belong to the IgSF fold, which consists of two anti-parallel β sheets linked together by an inter-sheet disulfide bond. The Ig fold has been grouped into three major sets: V set, C set and I set. The V and C sets originally were derived from antibody structure's variable and constant domains, respectively. The V set's two β sheets contain ABED and A′GFCC′C″ β strands, respectively, whereas the edge strands A′, C″ and C′ or D are missing in C set. I set is referred to as an intermediate set between V and C sets. Although, like a C set, topologically an I set is a truncation of V set, structurally it is close to V set. The key feature a V set and an I set share is that the A strand runs halfway down the domain in one sheet and kinks over at a *cis*-proline position to become A' strand, joining the opposite sheet by forming mainchain hydrogen bonds to the G strand in a parallel fashion (Harpaz and Chothia, 1994). Both D1 and D2 of these CAM molecules discussed here fall into I set of Ig fold category.

2. There are two unique characteristics of D1 structures of these CAM molecules. The first is an "extra" disulfide bond at the very tip of the molecule, between the BC loop and FG loop, not seen in any other IgSF structures. This disulfide bond brings these two otherwise widely open loops closed up and makes them impossible to serve as ligand-binding sites like their counterparts CDR1 and CDR3 antigen-combining loops in antibody do. The second is that an acidic residue that is known as the key integrin-binding residue is located either on the protruding CD loop (VCAM-1 and MAdCAM-1) or at the end of the C strand (ICAMs) near the bottom of the D1. Therefore, in contrast to antibodies and T cell receptors, the ligand-binding region of these CAMs is centered on the side of molecules' domain 1, but not at the top.

3. Structure-based mutation experiments have mapped the integrin-binding site on ICAM-2 domain 1 structure. The mapping applies to other ICAM family members as well. The site runs from the CD edge of the domain diagonally across the GFC β sheet (Casasnovas *et al.*, 1999). In the case of VCAM-1 and MAdCAM-1 the binding seems also to involve domain 2.

4. Although VCAM-1 and MAdCAM-1 differ from ICAMs in ligand-binding elements used and the type of integrins they interact (receptors for ICAMs are integrins with I domain, whereas those for VCAM-1 and MAdCAM-1 with no I domain), they all have an elaborate hydrogen bond networks around the key integrin-binding residues maintaining local conformation to facilitate binding.

5. Structure data suggested that each CAM molecule seems to evolve a special way to present its integrin-binding site in a proper orientation for recognition by an integrin on an opposing cell. ICAM-1, for example, appears to benefit from being a dimer on the cell surface. The dimeric ICAM-1 structure orients the key integrin-binding residue, Glu34, of domain 1 upwards for binding (Casasnovas *et al.*, 1998). On the other hand, ICAM-2 takes advantage of having three glycans on domain 2 forming a tripod-like architecture and retaining a relatively rigid D1-D2 bend to facilitate the key binding residue, Glu37, exposed (Casasnovas *et al.*, 1997).

Recently the first complex structure between binding domains of a CAM molecule and an integrin has revealed important features of how an IgSF molecule interacts with an integrin. This is the ICAM-1 D1–D3 fragment in complex with the $\alpha_L\beta_2$ I domain (Shimaoka *et al.*, 2003b) (Fig. 10, left panel). In the structure, the I domain has been engineered to introduce a disulfide bond that locks the I domain in an intermediately higher affinity compared to the wild type one. Several essential points are immediately apparent from the structure. First, domain 1 of ICAM-1 is exclusively engaged in binding, and there are no contacts between the ICAM-1 D2 and I domain. The ICAM-1 D1 docks onto I domain "top" face's shallow groove, with β strands on the D1 domain's CD edge parallel to the groove and roughly perpendicular to the central β sheet of the I domain. If one views the complex structure from ICAM-1 toward the I domain, the ICAM-1 D1's shadow would just cover the I domain. The key integrin-binding residue Glu34 at the end of C strand directly coordinates to the Mg^{2+} ion on the MADAS site at the groove's center. The binding does not induce any significant conformational changes in ICAM-1 molecule. Surrounding this Glu34, there is a ring of hydrophobic contact area between ICAM-1 and $\alpha_L\beta_2$. On the ICAM-1 side, the contributing residues include Pro36, Met64 and Tyr66, while on $\alpha_L\beta_2$ side these are Leu204, Leu205 and Met140. This non-polar environment around Glu34 should enforce the interaction between the Glu34 of ICAM-1 and Mg^{2+} ion on MIDAS, and provide major binding energy. Outside this hydrophobic ring are hydrophilic interactions. Apparently these interactions optimize the docking orientation. Of particular interests are many hydrogen bonds

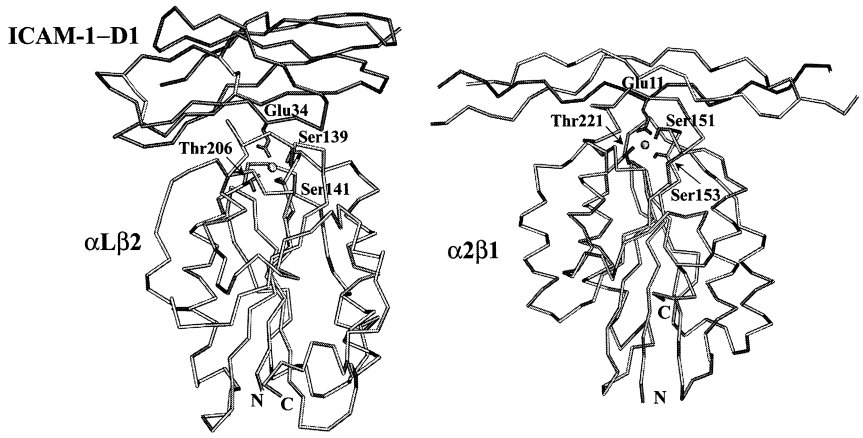

FIG. 10. Backbone diagram of two integrin/ligand complex structures. On the left panel is an intermediate affinity I domain from $\alpha_L\beta_2$ (in blue) in complex with ICAM-1 (in red). For clarity, only ICAM-1 D1 is shown. The sidechains of the key integrin-binding residue, Glu34, of ICAM-1 and MIDAS residues that directly coordinate the metal (in yellow) are illustrated. On the right panel is an I domain from $\alpha_2\beta_1$ (in blue) in complex with synthetic collagen-originated 21-mer triple-peptides (the major interacting middle strand is in red, and the other two strands are in yellow and green, respectively). Also, sidechains of the key integrin-binding residue, Glu11, of collagen and MIDAS residues of I domain are illustrated. The figure was prepared with SETOR. (See Color Insert.)

involving backbonds or sidechains that are conserved in ICAM family members. For example, the sidechain of the conserved Gln75 of ICAM-1 appears to make a pair of hydrogen bonds to sidechain of Asn207 of $\alpha_L\beta_2$ I domain. Another extremely interesting interaction is a salt bridge between Lys39 of ICAM-1 and Glu241 of I domain. The interaction can not take place without reorientation of Glu241 upon conversion of I domain from close to open conformation as described earlier. The Glu241 and the preceding Gly240 sit at the tip of a flexible $\beta4$-$\alpha5$ loop. Upon ligation, the I domain's Gly240 changes its dihedral angles from the β conformation to the area in Ramachadran map that only glycine is allowed. This glycine is conserved. The observation strongly suggests that the Gly240 facilitated swing of $\beta4$-$\alpha5$ loop and hence the sidechain of Glu241 appears to be crucial in switching the I domain into a high affinity state. The swing of the Glu241 and the resulting formation of the salt bridge of Glu241–Lys39 may be a general mechanism for regulating ligand binding by I domains.

B. E-Cadherin as Counter-Receptor

Cadherins are primary cell adhesion molecules responsible for Ca^{2+}-dependent cell–cell adhesion in vertebrate tissues. These transmembrane glycoproteins form a large cadherin superfamily. Depending on where they are mainly expressed, classical cadherins comprise E-, P-, N-, M- and VE-cadherin from epithelia, placenta, neurons, muscle and endothelial cells, respectively. Their extracellular portion consists of 5–6 cadherin folds, each being structurally related to an Ig fold (reviewed in Takeichi, 1990; Yagi and Takeichi, 2000). Crystal structures of domains of N- and E-cadherins are known (reviewed in Shapiro and Colman, 1998). More recently, the structure of an entire extracellular fragment of C-cadherin was reported (Boggon *et al.*, 2002). These structures showed how Ca^{2+} contributes to domain junction stability, and suggested a mechanism of homophilic adhesion.

E-cadherin is unique in that it not only, like other cadherin family members, mediates homophilic adhesion to establish and maintain cell-cell contacts, it also serves as a counter-receptor for integrins $\alpha_E\beta_7$ (Cepek *et al.*, 1994) and $\alpha_2\beta_1$ (Whittard *et al.*, 2002) in heterophilic adhesion. In fact, the interaction between E-cadherin on mucosal epithelial cells and $\alpha_E\beta_7$ on intraepithelial lymphocytes has been the best characterized tissue-specific interaction for lymphocyte retention. Although structure of binding domains between E-cadherin and $\alpha_E\beta_7$ is not available, mutagenesis data are informative of how these two molecules may interact (Higgins *et al.*, 2000; Taraszka *et al.*, 2000). Distinct from IgSF molecule described previously, E-cadherin's key integrin-binding residue, Glu31, is located on the N-terminal domain's BC loop at the very tip of the molecule (Fig. 9). Whereas this acidic residue coordinates metal ion on MADAS of $\alpha_E\beta_7$'s I domain, the sidechain of Phe298 in $\beta4$-$\alpha5$ loop from the I domain may extend into a hydrophobic pocket formed at E-cadherin's top part to strengthen binding.

C. Fibronectin as Counter-Receptor

Fibronectin (FN) is a large extracellular glycoprotein. It exists both as a soluble plasma protein and an aggregated fibril. The soluble plasma FN consists of two similar but not identical chains with molecular weight of 220–250 kDa each, joined together at their C-termini via two disulfide bonds. Each FN chain folds into 5–6 concatenate domains, each of which is specialized for binding to a particular molecule, such as collagen, heparin and integrin family member. Through these interactions, FN plays crucial roles in cell adhesion, cell morphology, cell migration,

thrombosis, hemostasis, etc. An individual domain can in turn be divided into smaller homologous modules of 40–90 residues, designated as type I, II, and III repeats. The 90-residue long FN-III repeats are the most common in FN, and are building units for many other proteins as well. In fact, the FN-III repeat is among the most common of all protein domains in vertebrates (for review, see Hynes, 1990; Schwarzbauer, 1991).

Structures of all three type FN modules are known. NMR data showed that FN-I and FN-II are both a small module of only 45 and 55 residues, respectively, with a few short β strands connected together by two disulfide bonds. The FN-I structure may suggest its binding surface to fibrin (Williams *et al.*, 1994). The known structures of FN-II modules were from metalloproteinase-2 (MMP-2) (Briknarova *et al.*, 2001; Gehrmann *et al.*, 2002). The structures have revealed enzyme's possible binding site for substrates (gelatin, laminin and other ECM proteins). FN-III has received much more attention from the structural biology community for the exploration of its integrin and other ligand binding properties. The first serious effort was from Erickson and his colleagues in their X-ray analyses of the third FN-III repeat alone (Leahy *et al.*, 1992) and later a four-repeat FN-III, the FN7-10 (Leahy *et al.*, 1996). Although with distinction, these structures have clearly illustrated the module's similar topology to the C set IgSF domain, having two facing β sheets of ABE and C′CFG but without the disulfide bond in between. A triplet sequence motif Arg-Gly-Asp (RGD) from the tenth FN-III was first discovered to be the key integrin-binding site for fibronectin (Pierschbacher and Ruoslahti, 1984).

Subsequently this RGD tripeptide was found in numerous adhesive proteins (fibrinogen, collagen, vitronectin, osteoponin, thrombospondin, etc.) present in ECM and blood, and identified to be a common integrin-recognition motif for these proteins (Ruoslahti and Pierschbacher, 1987). Crystal structure of FN7-10 depicted that the RGD motif is located on the tip of an unusually long and protruding FG loop of the 10th domain such that despite a rod-like contiguous abutting arrangement of the four FN-III modules, the RGD motif is 10 Å away from the molecule body and still well accessible for integrin-binding (Fig. 9). Apparently, having the glycine in place favors the RGD motif to be in a type II′ β turn, which may represent a general integrin-binding conformation (Leahy *et al.*, 1996). Another feature of the structure FN7-10 is that it suggests a synergy region on domain 9 aligning well with the RGD site on domain 10 on the same face of molecule. The two sites are separated by 30–40 Å, which should allow a single integrin molecule to interact simultaneously with both the RGD and the synergy region. More recently structure of FN12-14 suggests

a new class of integrin-binding sites (Sharma *et al.*, 1999). This is a sequence motif of Pro-Arg-Ala-Arg-Ile (PRARI) on FN14. The authors' speculation was based on: (1) This sequence PRARI in FN14 is at the same region as PHSRN sequence motif in FN9 that interact with integrins $\alpha_5\beta_1$ and $\alpha_{IIb}\beta_3$ in synergy with the RGD site in FN10; (2) Mutation of either arginine in PRARI motif to alanine impaired the integrin $\alpha_4\beta_1$ binding; (3) The PRARI motif is essentially conserved across all FN species. Since another ligand, heparin, binds to FN13 on a positively charged surface, which is on opposite face of integrin-binding site, the authors further hypothesized that loading or unloading heparin may facilitate integrin binding or *vice versa.*

Very recently, molecular electron microscopic image of a complex between the integrin $\alpha_5\beta_1$ headpiece and its physiological ligand, the FN7-10 fragment, for the first time has provided a view of how a protein ligand binds to an integrin (Takagi *et al.*, 2003b or #16024). The results convincingly demonstrate that the unliganded integrin is in a close conformation, and upon ligation the integrin transforms to an open conformation. The conformation changes are dramatic: the integrin's hybrid domain swings by 80° relative to the I-like domain in the β chain to let the large integrin molecule "stand up" from its bent state. The FN binding site is between the β-propeller and I-like domains of integrin headpiece. One interesting observation from this study is that it does not support the two-site binding mode. Their EM images and their kinetic analysis of $\alpha_5\beta_1$ binding to both wild type and mutant FN7-10 appear to suggest that the contribution of FN9's synergy site on to integrin-binding may only be an indirect one. In other words, the synergy site may just help orient the RGD loop on FN10 for binding and/or provide long-range electrostatic steering.

D. Collagen as Counter-Receptor

Collagens are a family of fibrous proteins present in all multicellular organisms. As a major component of skin and bone, they are the most abundant proteins in mammals, constituting about 25% of total protein mass. Their polypeptide chains have a regular $(\text{Gly-X-Y})_n$ sequence repeats, in which proline and 4-hydroxyproline frequently occupy the X and Y positions. This allows for three chains winding into a unique collagen helical structure with every third residue, the Gly, meeting in the center of three-helix bundle. Slightly different collagen chains assemble to create various type of collagens that either further polymerize to become collagen fibrillar or facilitate network-formation with other ECM proteins (see review Eyre, 1980).

Collagens as the major ECM proteins serve as counter-receptors for $\beta 1$ and $\beta 3$ integrins (Hynes, 1992). A specific collagen sequence motif Gly-Phe-HydroxyPro-Gly-Glu-Arg (GFOGER) has been identified as the integrin $\alpha_2\beta_1$ recognition site (Knight *et al.*, 2000). This finding stimulated the structure determination of a complex that contains the I domain from $\alpha_2\beta_1$ and a synthetic 21-mer peptide with the sequence of [Ac-$(GPO)_2$ GFOGER$(GPO)_3$-NH_2] that was shown to be in a triple helical conformation (Fig. 10, right panel) (Emsley *et al.*, 2000). In the structure, the authors named three collagen strands as "leading," "middle," and "trailing." The middle strand makes the majority of contacts with the I domain, whereas the trailing strand contributes fewer and the leading strand has no interactions. The key feature of the structure is the coordination of a glutamate sidechain of the middle strand to the metal ion on I domain's MADAS site. Like elaborated in preceding sections, three I domain metal-coordinating residues, Ser153, Ser155 and Thr221, lack a formal negative charge, which enables the metal ion to have strong bond to the collagen glutamate. One extremely interesting observation is that the collagen triple helical bundle also lies on a shallow groove of I domain with the collagen helical axis roughly perpendicular to the I domain's central β sheet, in a similar fashion as described for ICAM-1/$\alpha_L\beta_2$ complex structure. Aside from the key binding residue Glu, the neighboring residue Arg of the middle strand also participates in the specific interaction to Asp219 of I domain. The Arg of the trailing strand extends into a negatively charged well, close to a Glu256 of I domain. This Glu256 of $\alpha_2\beta_1$ is in an equivalent position as Glu241 of $\alpha_L\beta_2$ on the $\beta 4$-$\alpha 5$ loop, which undergoes the conformational flip upon ligation facilitated by a conserved Gly just one residue upstream from the Glu. It is worth mentioning again that in ICAM-1/$\alpha_L\beta_2$ binding domain complex structure, there is a salt bridge between this Glu from I domain to a Lys39 from ICAM-1. The Arg of the trailing strand, therefore, may well play a similar part as Lys39 does in ICAM-1/$\alpha_L\beta_2$ complex formation. It is not very clear what role another collagen residue, Phe, might play. Phe from the middle strand and trailing strand may just make hydrophobic contact to the I domain surface.

E. Fibrinogen as Counter-Receptor

Fibrinogen is a 340 kDa soluble glycoprotein found in the blood plasma of all vertebra animals. It functions *in vivo* as the precursor to an insoluble fibrin clot. Fibrinogen is a dimeric protein, with each protomer consisting

of three chains, Aα, Bβ, and γ. The dimer of hetero-trimer forms a long molecule of sigmoidal shape (Yang *et al.*, 2001). The β and γ chains each have a globular β structured domain at C-terminus. They combine to make up a D nodule. The two protomers meet at their N-termini with six chains interwinding into a small E nodule. D and E nodules are connected by a long coiled coil, which has four helices, two from hairpin-shaped α chain and one each from β and γ chains. That gives the molecule a size about 470Å long (Yang *et al.*, 2001).

The multi-functional fibrinogen also serves as ligand for β_2 and β_3 integrins. For instance, fibrinogen is the most abundant ligand for integrin $\alpha_{IIb}\beta_3$ on platelets, and the binding results in the formation of platelet-fibrin thrombi *in vivo* (Hawiger, 1994). The fibrinogen-binding sites on integrin $\alpha_{IIb}\beta_3$ map at the edge of the top and on the side of the β-propeller domain. The experiments were done by swapping predicted loops between α_{IIb} and other integrins such as α_4 or α_5, alanine scanning mutagenesis and molecular modeling (Kamata *et al.*, 2001). On the other hand, the integrin-binding site of fibrinogen has been mapped to the C-terminus of γ chain. The site encompasses residues γ400–γ411. The same segment also bears donor and acceptor sites for factor XIIIa-catalyzed cross-linking of fibrin (Chen and Doolittle, 1971). A crystal structure of a chimeric protein having this segment attached to the C-terminus of chicken egg white lysozyme gave a view of how this tail's conformation might look (Donahue *et al.*, 1994). A noticeable feature of the segment is to have two wide turns. In particular, one loop is stabilized by four hydrogen bonds through residue γGln399's sidechain to mainchain atoms contributed from γHis400–γHis401-γ Leu402–γGly403. It is likely that at least this part of structure may well represent the native structure in fibrinogen γ chain as a ligand for $\alpha_{IIb}\beta_3$, but not an artifact from the chimeric molecule.

Mutagenesis data have implied that the β_2 integrins $\alpha_M\beta_2$ and $\alpha_X\beta_2$ may share a common recognition site on fibrinogen, also located at γ chain on the D nodule. There are two sequence motifs on γ chain that are suggestive of involving β_2-binding: γ190–γ202 (P1 site) and γ377–γ395 (P2 site) (reviewed in Ugarova and Yakubenko, 2001). We noticed that within the D nodule, the γ chain C-terminal domain is at the two extremes of the elongated fibrinogen molecule, which may explain its functional importance for ligand-binding of both β_2 and β_3 integrins. There is no doubt that a complex structure between domains of integrin and fibrinogen is urgently needed to reveal this extremely important interaction.

F. Laminin as Counter-Receptor

Laminins are a family of large extracellular matrix glycoproteins. The best known family member is laminin-1, or classic laminin. Each laminin is a heterotrimer assembled from α, β and γ chains, secreted and incorporated with other matrix proteins (nidogen, type IV collagen and perlecan) into basement membranes. Basement membranes are thin layers of specialized extracellular matrices surrounding cells or separating layer of cells of different lineages. The basement membranes are fundamental to tissue organization and physiology in all metazoans. As a key component of basement membrane, laminins also bind to cell surface receptors, particularly integrins and dystroglycan, and the interactions control cellular activities (for review, see Colognato and Yurchenco, 2000).

A laminin heterotrimer appears in an asymmetric cross shape. Like many other matrix proteins, laminins' each chain has a modular architecture with tandem arrays of globular N-terminal domain (LN), rod-like EGF repeats (LE), globular domain IV (L4) and coiled coil region. In addition, the C-terminus of α chain has five G domain (LG) repeat (Engel *et al.*, 1981; Hohenester *et al.*, 1999). The receptor- and matrix-bindings of laminins are exerted by different regions of the molecules. The high-affinity interactions with nidogen within matrix is mediated through the LE modules 3–5 from γ1 chain domain III (Gerl *et al.*, 1991), particularly the module 4 (Mayer *et al.*, 1993). The crystal structures of this laminin fragment (Stetefeld *et al.*, 1996) and its complex to nidogen G3 domain, a β-propeller domain (Takagi *et al.*, 2003b), have been reported. Integrins that serve for laminin receptor fall into β_1 and β_4 subgroups. While $\alpha_1\beta_1$ and $\alpha_2\beta_1$ integrins' binding sites were found within the N-terminal LN domain of laminin's α chain short arm (Colognato *et al.*, 1997), other integrins, such as $\alpha_6\beta_1$, $\alpha_6\beta_4$ and $\alpha_7\beta_1$ bind to laminin's C-terminal LG domain (Aumailley *et al.*, 1990; Lee *et al.*, 1992; Song *et al.*, 1992). Crystal structure of LG5 from laminin α2 was determined (Hohenester *et al.*, 1999). This domain of about 200 residues folds into an anti-parallel β sandwich, reminiscent of a lectin fold. However, it was believed that the multi-functional ligand-binding sites of LG domain are distinct from lectins' carbohydrate-binding sites. Whereas the carbohydrate-binding sites of a lectin cluster on the concave surface of the β sandwich, the LG domain may offer the rim of the β sandwich as its ligand-binding region, similar to antibody's antigen combining loops (Rudenko *et al.*, 2001). It is interesting to observe from the crystal structure that a calcium cation is bound to one edge of the sandwich by conserved acidic residues, and a sulfate ion has been identified in the structure to take part in calcium coordination, a mimic of ligand-binding. The cation-binding edge is on

the opposite side of where the N- and C-termini of the LG domain meet (Hohenester *et al.*, 1999), which appears ideal for binding to ligands, probably also including integrins. So far there are no further experimental data available about how laminin and integrin interact.

References

Alonso, J. L., Essafi, M., Xiong, J. P., Stehle, T., and Arnaout, M. A. (2002). Does the integrin αA domain act as a ligand for its βA domain? *Curr. Biol.* **12,** R340–R342.

Aumailley, M., Timpl, R., and Sonnenberg, A. (1990). Antibody to integrin α6 subunit specifically inhibits cell-binding to laminin fragment 8. *Exper. Cell Res.* **188,** 55–60.

Beglova, N., Blacklow, S. C., Takagi, J., and Springer, T. A. (2002). Cysteine-rich module structure reveals a fulcrum for integrin rearrangement upon activation. *Nat. Struct. Biol.* **9,** 282–287.

Billheimer, J. T., Dicker, I. B., Wynn, R., Bradley, J. D., Cromley, D. A., Godonis, H. E., Grimminger, L. C., He, B., Kieras, C. J., and Pedicord, D. L. *et al.* (2002). Evidence that thrombocytopenia observed in humans treated with orally bioavailable glycoprotein IIb/IIIa antagonists is immune mediated. *Blood* **99,** 1–7.

Boggon, T. J., Murray, J., Chappuis-Flament, S., Wong, E., Gumbiner, B. M., and Shapiro, L. (2002). C-cadherin ectodomain structure and implications for cell adhesion mechanisms. *Science* **296,** 1308–1313.

Briknarova, K., Gehrmann, M., Banyai, L., Tordai, H., Patthy, L., and Llinas, M. (2001). Gelatin-binding region of human matrix metalloproteinase-2: Solution structure, dynamics, and function of the COL-23 two-domain construct. *J. Biol. Chem.* **276,** 27613–27621.

Carson, M. (1997). Ribbons. *Methods Enzymol.* **277,** 493–505.

Casasnovas, J., Pieroni, C., and Springer, T. A. (1999). Lymphocyte function-associated antigen-1 binding residues in intercellular adhesion molecule-2 (ICAM-2) and the integrin binding surface in the ICAM subfamily. *Proc. Natl. Acad. Sci. USA* **96,** 3017–3022.

Casasnovas, J. M., Springer, T. A., Liu, J.-h., Harrison, S. C., and Wang, J.-h. (1997). The crystal structure of ICAM-2 reveals a distinctive integrin recognition surface. *Nature* **387,** 312–315.

Casasnovas, J. M., Stehle, T., Liu, J.-h., Wang, J.-h., and Springer, T. A. (1998). A dimeric crystal structure for the N-terminal two domains of ICAM-1. *Proc. Natl. Acad. Sci. USA* **95,** 4134–4139.

Cepek, K. L., Shaw, S. K., Parker, C. M., Russell, G. J., Morrow, J. S., Rimm, D. L., and Brenner, M. B. (1994). Adhesion between epithelial cells and T lymphocytes mediated by E-cadherin and the αEβ7 integrin. *Nature* **372,** 190–193.

Chen, J. F., Salas, A., and Springer, T. A. (2003). Bistable regulation of integrin adhesiveness by a bipolar metal ion cluster. *Nat. Struct. Biol.* **10,** 995–1001.

Chen, R., and Doolittle, R. F. (1971). Cross-linking sites in human and bovine fibrin. *Biochemistry* **10,** 4487–4491.

Colognato, H., MacCarrick, M., O'Rear, J. J., and Yurchenco, P. D. (1997). The laminin α2-chain short arm mediates cell adhesion through both the α1β1 and α2β1 integrins. *J. Biol. Chem.* **272,** 29330–29336.

Colognato, H., and Yurchenco, P. D. (2000). Form and function: The laminin family of heterotrimers. *Dev. Dyn.* **218,** 213–234.

Curley, G. P., Blum, H., and Humphries, M. J. (1999). Integrin antagonists. *Cell Mol. Life Sci.* **56,** 427–441.

de Pereda, J. M., Wiche, G., and Liddington, R. C. (1999). Crystal structure of a tandem pair of fibronectin type III domains from the cytoplasmic tail of integrin $\alpha 6\beta 4$. *EMBO J.* **18,** 4087–4095.

Diamond, M. S., Garcia-Aguilar, J., Bickford, J. K., Corbi, A. L., and Springer, T. A. (1993). The I domain is a major recognition site on the leukocyte integrin Mac-1 (CD11b/CD18) for four distinct adhesion ligands. *J. Cell. Biol.* **120,** 1031–1043.

Donahue, J. P., Patel, H., Anderson, W. F., and Hawiger, J. (1994). Three-dimensional structure of the platelet integrin recognition segment of the fibrinogen γ chain obtained by carrier protein-driven crystallization. *Proc. Natl. Acad. Sci. USA* **91,** 12178–12182.

Du, X., Gu, M., Weisel, J. W., Nagaswami, C., Bennett, J. S., Bowditch, R., and Ginsberg, M. H. (1993). Long range propagation of conformational changes in integrin $\alpha_{IIb}\beta_3$. *J. Biol. Chem.* **268,** 23087–23092.

Du, X., Plow, E. F., Frelinger, A. L., III, O'Toole, T. E., Loftus, J. C., and Ginsberg, M. H. (1991). Ligands "activate" integrin αIIbβ3 (platelet GPIIb-IIIa). *Cell* **65,** 409–416.

Emsley, J., Knight, C. G., Farndale, R. W., Barnes, M. J., and Liddington, R. C. (2000). Structural basis of collagen recognition by integrin $\alpha 2\beta 1$. *Cell* **101,** 47–56.

Engel, J., Odermatt, E., Engel, A., Madri, J. A., Furthmayr, H., Rohde, H., and Timpl, R. (1981). Shapes, domain organizations and flexibility of laminin and fibronectin, two multifunctional proteins of the extracellular matrix. *J. Mol. Biol.* **150,** 97–120.

Eyre, D. R. (1980). Collagen: Molecular diversity in the body's protein scaffold. *Science* **207,** 1315–1322.

Garcia-Alvarez, B., de Pereda, J. M., Calderwood, D. A., Ulmer, T. S., Critchley, D., Campbell, I. D., Ginsberg, M. H., and Liddington, R. C. (2003). Structural determinants of integrin recognition by talin. *Mol. Cell* **11,** 49–58.

Gehrmann, M., Briknarova, K., Banyai, L., Patthy, L., and Llinas, M. (2002). The col-1 module of human matrix metalloproteinase-2 (MMP-2): Structural/functional relatedness between gelatin-binding fibronectin type II modules and lysine-binding kringle domains. *Biol. Chem.* **383,** 137–148.

Gerl, M., Mann, K., Aumailley, M., and Timpl, R. (1991). Localization of a major nidogen-binding site to domain III of laminin B2 chain. *Eur. J. Biochem.* **202,** 167–174.

Giblin, P. A., and Kelly, T. A. (2001). Antagonists of $\beta 2$ integrin-mediated cell adhesion. *Annu. Rep. Med. Chem.* **36,** 181–190.

Gordon, K. B., Papp, K. A., Hamilton, T. K., Walicke, P. A., Dummer, W., Li, N., Bresnahan, B. W., and Menter, A. (2003). Efalizumab for patients with moderate to severe plaque psoriasis: A randomized controlled trial. *Jama* **290,** 3073–3080.

Harpaz, Y., and Chothia, C. (1994). Many of the immoglobulin superfamily domains in cell adhesion molecules and surface receptors belong to a new structural set which is close to that containing variable domains. *J. Mol. Biol.* **238,** 528–539.

Hawiger, J. (1994). *In* "Hemostasis and Thrombosis: Basic Principles and Clinical Practice", (R. W. Colman, J. Hirsch, V. J. Marder, and E. W. Salzman, Eds.), pp. 762. Lippincot, PA.

Higgins, J. M., Cernadas, M., Tan, K., Irie, A., Wang, J., Takada, Y., and Brenner, M. B. (2000). The role of α and β chains in ligand recognition by $\beta 7$ integrins. *J. Biol. Chem.* **275,** 25652–25664.

Hohenester, E., Tisi, D., Talts, J. F., and Timpl, R. (1999). The crystal structure of a laminin G-like module reveals the molecular basis of α-dystroglycan binding to laminins, perlecan, and agrin. *Mol. Cell* **4,** 783–792.

Huang, C., Zang, Q., Takagi, J., and Springer, T. A. (2000). Structural and functional studies with antibodies to the integrin β2 subunit: A model for the I-like domain. *J. Biol. Chem.* **275,** 21514–21524.

Humphries, M. J. (2000). Integrin structure. *Biochem. Soc. Trans.* **28,** 311–339.

Huth, J. R., Olejniczak, E. T., Mendoza, R., Liang, H., Harris, E. A., Lupher, M. L., Jr., Wilson, A. E., Fesik, S. W., and Staunton, D. E. (2000). NMR and mutagenesis evidence for an I domain allosteric site that regulates lymphocyte function-associated antigen 1 ligand binding. *Proc. Natl. Acad. Sci. USA* **97,** 5231–5236.

Hynes, R. (1990). Fibronectins. Springer-Verlag, New York.

Hynes, R. O. (1992). Integrins: Versatility, modulation, and signaling in cell adhesion. *Cell* **69,** 11–25.

Hynes, R. O., and Zhao, Q. (2000). The evolution of cell adhesion. *J. Cell. Biol.* **150,** F89–F96.

Kallen, J., Welzenbach, K., Ramage, P., Geyl, D., Kriwacki, R., Legge, G., Cottens, S., Weitz-Schmidt, G., and Hommel, U. (1999). Structural basis for LFA-1 inhibition upon lovastatin binding to the CD11a I-domain. *J. Mol. Biol.* **292,** 1–9.

Kamata, T., Tieu, K. K., Springer, T. A., and Takada, Y. (2001). Amino acid residues in the αIIb subunit that are critical for ligand binding to integrin αIIbβ3 are clustered in the β-propeller model. *J. Biol. Chem.* **276,** 44275–44283.

Kim, M., Carman, C. V., and Springer, T. A. (2003). Bidirectional transmembrane signaling by cytoplasmic domain separation in integrins. *Science* **301,** 1720–1725.

Kim, M., Carman, C. V., Yang, W., Salas, A., and Springer, T. A. (2004). LFA-1 clustering occurs as a consequence of, rather than a prelude to, cell adhesion. In preparation.

Knight, C. G., Morton, L. F., Peachey, A. R., Tuckwell, D. S., Farndale, R. W., and Barnes, M. J. (2000). The collagen-binding A-domains of integrins α1β1 and α2β1 recognize the same specific amino acid sequence, GFOGER, in native (triple-helical) collagens. *J. Biol. Chem.* **275,** 35–40.

Kouns, W. C., Kirchhofer, D., Hadvary, P., Edenhofer, A., Weller, T., Pfenninger, G., Baumgartner, H. R., Jennings, L. K., and Steiner, B. (1992). Reversible conformational changes induced in glycoprotein IIb-IIIa by a potent and selective peptidomimetic inhibitor. *Blood* **80,** 2539–2547.

Leahy, D. J., Aukhil, I., and Erickson, H. P. (1996). 2.0 angstrom crystal structure of a four-domain segment of human fibronectin encompassing the RGD Loop and synergy region. *Cell* **84,** 155–164.

Leahy, D. J., Hendrickson, W. A., Aukhil, I., and Erickson, H. P. (1992). Structure of a fibronectin type III domain from tenascin phased by MAD analysis of the selenomethionyl protein. *Science* **258,** 987–991.

Lee, E. C., Lotz, M. M., Steele, G. D. J., and Mercurio, A. M. (1992). The integrin $\alpha_6\beta_4$ is a laminin receptor. *J. Cell Biol.* **117,** 671–678.

Lee, J.-O., Bankston, L. A., Arnaout, M. A., and Liddington, R. C. (1995a). Two conformations of the integrin A-domain (I-domain): A pathway for activation? *Structure* **3,** 1333–1340.

Lee, J.-O., Rieu, P., Arnaout, M. A., and Liddington, R. (1995b). Crystal structure of the A domain from the α subunit of integrin CR3 (CD11b/CD18). *Cell* **80,** 631–638.

Li, R., Babu, C. R., Lear, J. D., Wand, A. J., Bennett, J. S., and Degrado, W. F. (2001). Oligomerization of the integrin αIIbβ3: Roles of the transmembrane and cytoplasmic domains. *Proc. Natl. Acad. Sci. USA* **98,** 12462–12467.

Li, R., Mitra, N., Gratkowski, H., Vilaire, G., Litvinov, S. V., Nagasami, C., Weisel, J. W., Lear, J. D., DeGrado, W. F., and Bennett, J. S. (2003). Activation of integrin αIIbβ3 by modulation of transmembrane helix associations. *Science* **300,** 795–798.

Lu, C., Ferzly, M., Takagi, J., and Springer, T. A. (2001a). Epitope mapping of antibodies to the C-terminal region of the integrin β2 subunit reveals regions that become exposed upon receptor activation. *J. Immunol.* **166,** 5629–5637.

Lu, C., Shimaoka, M., Ferzly, M., Oxvig, C., Takagi, J., and Springer, T. A. (2001b). An isolated, surface-expressed I domain of the integrin αLβ2 is sufficient for strong adhesive function when locked in the open conformation with a disulfide. *Proc. Natl. Acad. Sci. USA* **98,** 2387–2392.

Lu, C., Shimaoka, M., Zang, Q., Takagi, J., and Springer, T. A. (2001c). Locking in alternate conformations of the integrin αLβ2 I domain with disulfide bonds reveals functional relationships among integrin domains. *Proc. Natl. Acad. Sci. USA* **98,** 2393–2398.

Lu, C., Takagi, J., and Springer, T. A. (2001d). Association of the membrane-proximal regions of the α and β subunit cytoplasmic domains constrains an integrin in the inactive state. *J. Biol. Chem.* **276,** 14642–14648.

Luo, B.-H., Springer, T. A., and Takagi, J. (2003a). High affinity ligand binding by integrins does not involve head separation. *J. Biol. Chem.* **278,** 17185–17189.

Luo, B.-H., Springer, T. A., and Takagi, J. (2003b). Stabilizing the open conformation of the integrin headpiece with a glycan wedge increases affinity for ligand. *PNAS* **100,** 2403–2408.

Luo, B.-H., Springer, T. A., and Takagi, J. (2004a). A specific interface between integrin transmembrane helices and affinity for ligand. *Pub. Lib. Sci.* **2,** E113.

Luo, B.-H., Takagi, J., and Springer, T. A. (2004b). Locking the β3 integrin I-like domain into high and low affinity conformations with disulfides. *J. Biol. Chem.* **279,** 10215–10221.

Mayer, U., Nischt, R., Poschl, E., Mann, K., Fukuda, K., Gerl, M., Yamada, Y., and Timpl, R. (1993). A single EGF-like motif of laminin is responsible for high affinity nidogen binding. *EMBO J.* **12,** 1879–1885.

Michishita, M., Videm, V., and Arnaout, M. A. (1993). A novel divalent cation-binding site in the A domain of the β2 integrin CR3 (CD11b/CD18) is essential for ligand binding. *Cell* **72,** 857–867.

Mould, A. P., Askari, J. A., Barton, S., Kline, A. D., McEwan, P. A., Craig, S. E., and Humphries, M. J. (2002). Integrin activation involves a conformational change in the α1 helix of the β subunit A-domain. *J. Biol. Chem.* **277,** 19800–19805.

Mould, A. P., Barton, S. J., Askari, J. A., Craig, S. E., and Humphries, M. J. (2003a). Role of ADMIDAS cation-binding site in ligand recognition by integrin α5β1. *J. Biol. Chem.* **278,** 51622–51629.

Mould, A. P., Barton, S. J., Askari, J. A., McEwan, P. A., Buckley, P. A., Craig, S. E., and Humphries, M. J. (2003b). Conformational changes in the integrin βA domain provide a mechanism for signal transduction via hybrid domain movement. *J. Biol. Chem.* **278,** 17028–17035.

Mould, A. P., Symonds, E. J., Buckley, P. A., Grossmann, J. G., McEwan, P. A., Barton, S. J., Askari, J. A., Craig, S. E., Bella, J., and Humphries, M. J. (2003c). Structure of an integrin-ligand complex deduced from solution x-ray scattering and site-directed mutagenesis. *J. Biol. Chem.* **278,** 39993–39999.

Pierschbacher, M. D., and Ruoslahti, E. (1984). Cell attachment activity of fibronectin can be duplicated by small synthetic fragments of the molecule. *Nature* **309,** 30–33.

Puzon-McLaughlin, W., Kamata, T., and Takada, Y. (2000). Multiple discontinuous ligand-mimetic antibody binding sites define a ligand binding pocket in integrin αIIbβ3. *J. Biol. Chem.* **275,** 7795–7802.

Rudenko, G., Hohenester, E., and Muller, Y. A. (2001). LG/LNS domains: Multiple functions—one business end? *Trends Biochem. Sci.* **26,** 363–368.

Ruoslahti, E., and Pierschbacher, M. D. (1987). New perspectives in cell adhesion: RGD and integrins. *Science* **238,** 491–497.

Salas, A., Shimaoka, M., Chen, S., Carman, C. V., and Springer, T. A. (2002). Transition from rolling to firm adhesion is regulated by the conformation of the I domain of the integrin LFA-1. *J. Bio. Chem.* **277,** 50255–50262.

Salas, A., Shimaoka, M., Kogan, A. N., Harwood, C., von Andrian, U. H., and Springer, T. A. (2004). Rolling adhesion through an extended conformation of integrin αLβ2 and relation to α I and β I-like domain interaction. *Immunity* In press.

Scarborough, R. M., and Gretler, D. D. (2000). Platelet glycoprotein IIb-IIIa antagonists as prototypical integrin blockers: Novel parenteral and potential oral antithrombotic agents. *J. Med. Chem.* **43,** 3453–3473.

Schwarzbauer, J. E. (1991). Fibronectin: From gene to protein. *Curr. Opin. Cell Biol.* **3,** 786–791.

Shapiro, L., and Colman, D. R. (1998). Structural biology of cadherins in the nervous system. *Curr. Opin. Neurobiol.* **8,** 593–599.

Sharma, A., Askari, J. A., Humphries, M. J., Jones, E. Y., and Stuart, D. I. (1999). Crystal structure of a heparin- and integrin-binding segment of human fibronectin. *EMBO J.* **18,** 1468–1479.

Shimaoka, M., Lu, C., Palframan, R., von Andrian, U. H., Takagi, J., and Springer, T. A. (2001). Reversibly locking a protein fold in an active conformation with a disulfide bond: Integrin αL I domains with high affinity and antagonist activity *in vivo*. *Proc. Natl. Acad. Sci. USA* **98,** 6009–6014.

Shimaoka, M., Salas, A., Yang, W., Weitz-Schmidt, G., and Springer, T. A. (2003a). Small molecule integrin antagonists that bind to the β2 subunit I-like domain and activate signals in one direction and block them in another. *Immunity* **19,** 391–402.

Shimaoka, M., and Springer, T. A. (2003). Therapeutic antagonists and the conformational regulation of integrin structure and function. *Nat. Rev. Drug. Disc.* **2,** 703–716.

Shimaoka, M., Takagi, J., and Springer, T. A. (2002). Conformational regulation of integrin structure and function. *Annu. Rev. Biophys. Biomol. Struct.* **31,** 485–516.

Shimaoka, M., Xiao, T., Liu, J.-H., Yang, Y., Dong, Y., Jun, C.-D., McCormack, A., Zhang, R., Joachimiak, A., and Takagi, J. *et al.* (2003b). Structures of the αL I domain and its complex with ICAM-1 reveal a shape-shifting pathway for integrin regulation. *Cell* **112,** 99–111.

Song, W. K., Wang, W., Foster, R. F., Bielser, D. A., and Kaufman, S. J. (1992). H36-α7 is a novel integrin α chain that is developmentally regulated during skeletal myogenesis. *J. Cell. Biol.* **117,** 643–657.

Springer, T. A. (1994). Traffic signals for lymphocyte recirculation and leukocyte emigration: The multi-step paradigm. *Cell* **76,** 301–314.

Springer, T. A. (1997). Folding of the N-terminal, ligand-binding region of integrin α-subunits into a β-propeller domain. *Proc. Natl. Acad. Sci. USA* **94,** 65–72.

Stetefeld, J., Mayer, U., Timpl, R., and Huber, R. (1996). Crystal structure of three consecutive laminin-type epidermal growth factor-like (LE) modules of laminin γ1 chain harboring the nidogen binding site. *J. Mol. Biol.* **257,** 644–657.

Takagi, J., Erickson, H. P., and Springer, T. A. (2001). C-terminal opening mimics "inside-out" activation of integrin $\alpha 5\beta 1$. *Nature Struct. Biol.* **8,** 412–416.

Takagi, J., Kamata, T., Meredith, J., Puzon-McLaughlin, W., and Takada, Y. (1997). Changing ligand specificities of $\alpha v\beta 1$ and $\alpha v\beta 3$ integrins by swapping a short diverse sequence of the β subunit. *J. Biol. Chem.* **272,** 19794–19800.

Takagi, J., Petre, B. M., Walz, T., and Springer, T. A. (2002). Global conformational rearrangements in integrin extracellular domains in outside-in and inside-out signaling. *Cell* **110,** 599–611.

Takagi, J., and Springer, T. A. (2002). Integrin activation and structural rearrangement. *Immunological Rev.* **186,** 141–163.

Takagi, J., Strokovich, K., Springer, T. A., and Walz, T. (2003a). Structure of integrin $\alpha 5\beta 1$ in complex with fibronectin. *EMBO J.* **22,** 4607–4615.

Takagi, J., Yang, Y., Liu, J.-h., Wang, J.-h., and Springer, T. A. (2003b). Complex between nidogen and laminin fragments reveals a paradigmatic β-propeller interface. *Nature* **424,** 969–974.

Takeichi, M. (1990). Cadherins: A molecular family important in selective cell-cell adhesion. *Annu. Rev. Biochem.* **59,** 237–252.

Taraszka, K. S., Higgins, J. M., Tan, K., Mandelbrot, D. A., Wang, J. H., and Brenner, M. B. (2000). Molecular basis for leukocyte integrin $\alpha E\beta 7$ adhesion to epithelial (E)-cadherin. *J. Exp. Med.* **191,** 1555–1567.

Ugarova, T. P., and Yakubenko, V. P. (2001). Recognition of fibrinogen by leukocyte integrins. *Ann. NY Acad. Sci.* **936,** 365–385.

Varner, J. A., and Cheresh, D. A. (1996). Tumor angiogenesis and the role of vascular cell integrin $\alpha v\beta 3$. *Important Adv. Oncol.* 69–87.

Vinogradova, O., Velyvis, A., Velyviene, A., Hu, B., Haas, T. A., Plow, E. F., and Qin, J. (2002). A structural mechanism of integrin $\alpha_{IIb}\beta_3$ "inside-out" activation as regulated by its cytoplasmic face. *Cell* **110,** 587–597.

Wang, J.-h., and Springer, T. A. (1998). Structural specializations of immunoglobulin superfamily members for adhesion to integrins and viruses. *Immunol. Rev.* **163,** 197–215.

Weisel, J. W., Nagaswami, C., Vilaire, G., and Bennett, J. S. (1992). Examination of the platelet membrane glycoprotein IIb-IIIa complex and its interaction with fibrinogen and other ligands by electron microscopy. *J. Biol. Chem.* **267,** 16637–16643.

Weljie, A. M., Hwang, P. M., and Vogel, H. J. (2002). Solution structures of the cytoplasmic tail complex from platelet α IIb- and β 3-subunits. *Proc. Natl. Acad. Sci. USA* **99,** 5878–5883.

Whittard, J. D., Craig, S. E., Mould, A. P., Koch, A., Pertz, O., Engel, J., and Humphries, M. J. (2002). E-cadherin is a ligand for integrin $\alpha 2\beta 1$. *Matrix Biol.* **21,** 525–532.

Williams, M. J., Phan, I., Harvey, T. S., Rostagno, A., Gold, L. I., and Campbell, I. D. (1994). Solution structure of a pair of fibronectin type 1 modules with fibrin binding activity. *J. Mol. Biol.* **235,** 1302–1311.

Woska, J. R., Jr., Shih, D., Taqueti, V. R., Hogg, N., Kelly, T. A., and Kishimoto, T. K. (2001). A small-molecule antagonist of LFA-1 blocks a conformational change important for LFA-1 function. *J. Leukoc. Biol.* **70,** 329–334.

Xiong, J.-P., Stehle, T., Diefenbach, B., Zhang, R., Dunker, R., Scott, D. L., Joachimiak, A., Goodman, S. L., and Arnaout, M. A. (2001). Crystal structure of the extracellular segment of integrin $\alpha V\beta 3$. *Science* **294,** 339–345.

Xiong, J. P., Stehle, T., Zhang, R., Joachimiak, A., Frech, M., Goodman, S. L., and Arnaout, M. A. (2002). Crystal structure of the extracellular segment of integrin $\alpha V\beta 3$ in complex with an Arg-Gly-Asp ligand. *Science* **296,** 151–155.

Yagi, T., and Takeichi, M. (2000). Cadherin superfamily genes: Functions, genomic organization, and neurologic diversity. *Genes Dev.* **14,** 1169–1180.

Yang, W., Shimaoka, M., Chen, J. F., and Springer, T. A. (2004a). Activation of integrin β subunit I-like domains by one-turn C-terminal α-helix deletions. *Proc. Natl. Acad. Sci. USA* **101,** 2333–2338.

Yang, W., Shimaoka, M., Salas, A., Takagi, J., and Springer, T. A. (2004b). Inter-subunit signal transmission in integrins by a receptor-like interaction with a pull spring. *Proc. Natl. Acad. Sci. USA* **101,** 2906–2911.

Yang, Z., Kollman, J. M., Pandi, L., and Doolittle, R. F. (2001). Crystal structure of native chicken fibrinogen at 2.7 A resolution. *Biochemistry* **40,** 12515–12523.

Yusuf-Makagiansar, H., Anderson, M. E., Yakovleva, T. V., Murray, J. S., and Siahaan, T. J. (2002). Inhibition of LFA-1/ICAM-1 and VLA-4/VCAM-1 as a therapeutic approach to inflammation and autoimmune diseases. *Med. Res. Rev.* **22,** 146–167.

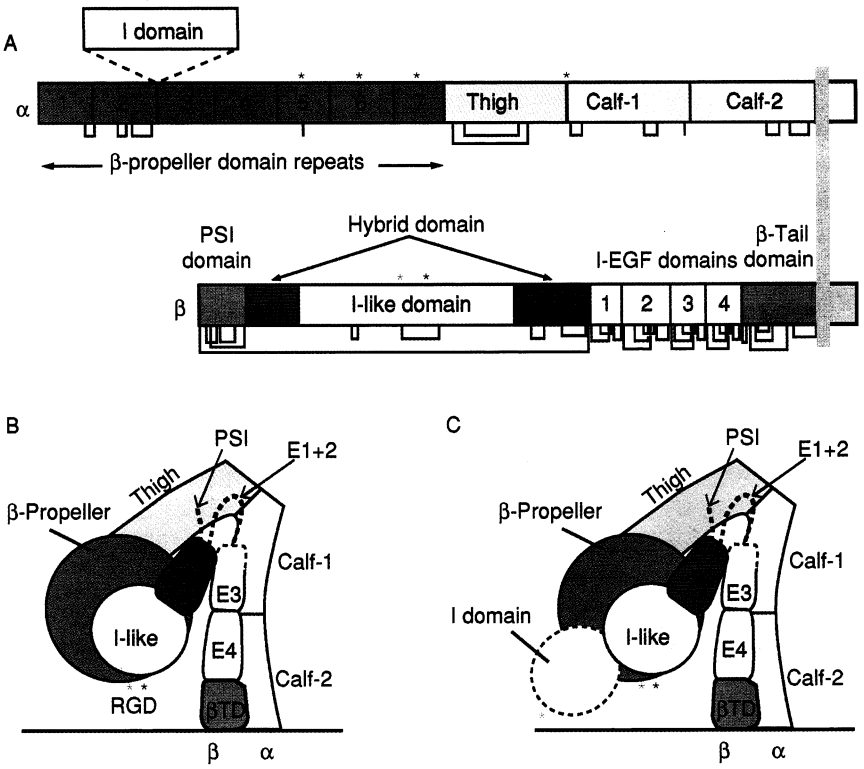

SPRINGER AND WANG, FIG. 2. Integrin architecture. (A) Organization of domains within the primary structure. Some α subunits contain an I domain inserted in the position denoted by the dotted lines. Cysteines and disulfide bonds are shown as lines below the stick figures. Red and blue asterisks denote Ca^{2+} and Mg^{2+} binding sites, respectively. (B) Arrangement of domains within the three-dimensional crystal structure of $\alpha_v\beta_3$ (Xiong *et al.*, 2001). Each domain is color coded as in A. (C) The structure in (B) with an I domain added.

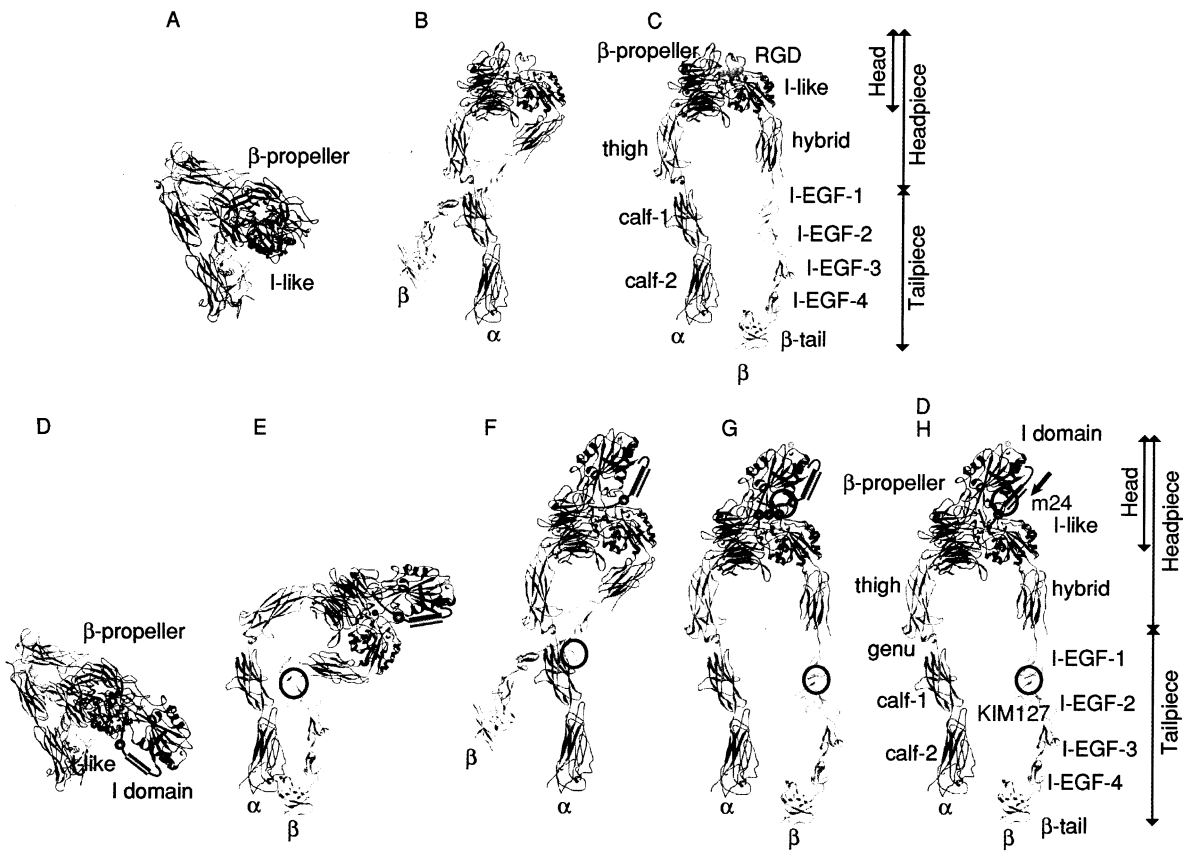
A
β-propeller
I-like
B
β
α
C
β-propeller
RGD
I-like
thigh
hybrid
I-EGF-1
calf-1
I-EGF-2
I-EGF-3
calf-2
I-EGF-4
β-tail
α
β
Head
Headpiece
Tailpiece
D
β-propeller
I-like
I domain
E
α
β
F
β
α
G
α
β
D
H
I domain
β-propeller
m24
I-like
thigh
hybrid
genu
I-EGF-1
calf-1
KIM127
I-EGF-2
calf-2
I-EGF-3
I-EGF-4
β-tail
α
β
Head
Headpiece
Tailpiece

SPRINGER AND WANG, FIG. 3. Conformational states for integrins. A–C. Model for $\alpha_v\beta_3$ integrin activation, with at least three conformations of the extracellular domain (Takagi *et al.*, 2002). (A) Bent, low affinity conformation. (B) Extended conformation with closed headpiece. (C) Extended conformation with open headpiece shown with bound RGD-mimetic peptide (green CPK). D–H. Model for $\alpha_L\beta_2$ integrin activation. (D) Bent conformation with low affinity. (E) and (F) $\alpha_L\beta_2$ with a closed headpiece and closed I domain in partially (E) or fully (F) extended states. (G) Extended conformation with open headpiece, and closed I domain, in the presence of α/β I-like allosteric antagonist, represented by three red spheres. (H) Extended conformation with open headpiece and open I domain. The models for all of the extracellular domains except for the I domain are based on conformational states of $\alpha_v\beta_3$ defined by negative stain electron microscopy (Takagi *et al.*, 2002), crystallography (Xiong *et al.*, 2002), NMR (Beglova *et al.*, 2002), and mapping of activation epitopes (Lu *et al.*, 2001a,c). The α_L I domain is a cartoon based on crystal structures (Shimaoka *et al.*, 2003b). The I domain is joined at the point of its insertion in the β-propeller domain but its orientation is arbitrary; it is shown at slightly larger scale for emphasis. The C-terminal I domain α-helix is represented by a red cylinder, and α_L Glu-310 in the linker as a blue sphere. The positions of activation epitopes m24 and KIM127 are circled only in the conformations in which they are thought to be exposed.

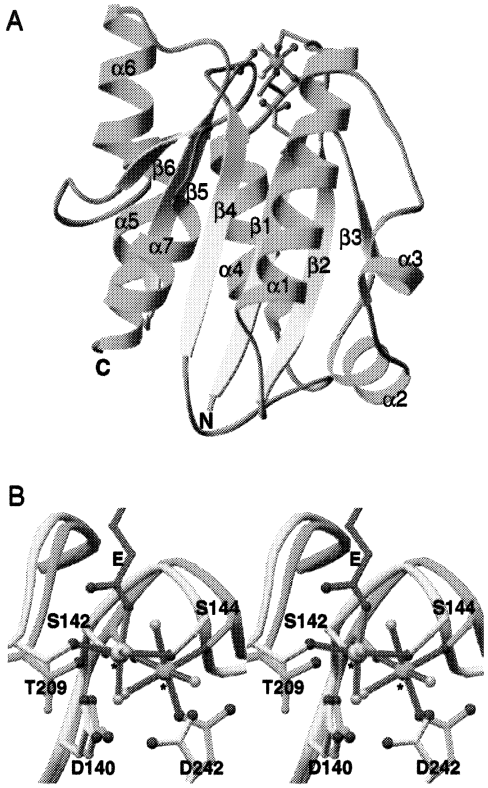

SPRINGER AND WANG, FIG. 4. α I domain structure and MIDAS conformational change. (A) Ribbon diagram of the α_M I domain in the open conformation (Lee *et al.*, 1995b). The β-strands (yellow), α-helices (cyan), and the N and C termini are labeled. The Mg ion is shown as a green sphere, and primary coordination bonds are blue. Side chains of residues that form primary or secondary coordinations to the metal ion are shown with grey bonds and carbon atoms and red oxygen atoms, and the oxygen of the ligand-mimetic Glu from another I domain is magenta. Coordinating water molecule oxygens are gold. Prepared with Ribbons (Carson, 1997). (B) Stereo view of alternative conformations of the α_M MIDAS. The backbone, coordinating side chain bonds, and metals (labeled with asterisks) are shown in yellow (open conformation) and cyan (closed conformation). The coordinating glutamate residue from the ligand-mimetic neighboring α_M I domain in α_M is in magenta. Primary coordination bonds to the metals are in blue. Oxygen atoms of the coordinating side chains and water molecules are red and gold, respectively. The 1IDO open α_M structure (Lee *et al.*, 1995a) was superimposed on the closed 1JLM α_M structure (Lee *et al.*, 1995b) using residues 132–141, 166–206, 211–241, 246–270, and 287–294.

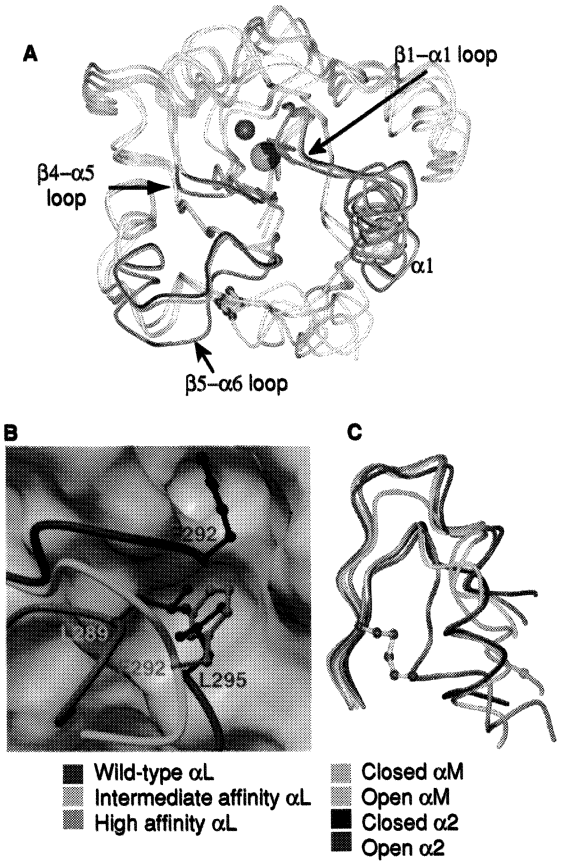

SPRINGER AND WANG, FIG. 5. Propagation of conformational change in the I domain. (A) The structures of the unliganded wild type, intermediate affinity, and high affinity αL I domains (Shimaoka *et al.*, 2003b). The three unliganded αL I domain backbones are shown superimposed and viewed centered on the MIDAS. Regions of the backbones that differ structurally are labeled and color keyed; other backbone regions are grey. The metal ions at the MIDAS and the atoms in the mutationally introduced, disulfide linked cysteine atoms are shown in the same colors as the backbone regions that differ; the cysteine sidechain bonds are yellow. The position of the missing metal ion in the high affinity structure is simulated with a smaller sphere. β6-α7 loop and α7 are shown in grey for clarity; differences in these regions are shown in (B) and (C). (B) The hydrophobic pocket that acts as a detent for the rachet-like movement of the β6-α7 loop. The backbone of the β6-α7 loop and the three residues that occupy the same hydrophobic pocket in the three different conformational states are color keyed. The pocket is shown as a GRASP van der Waals surface using the wild-type 1LFA structure with the residues from 287 to the C-terminus deleted. The upper hydrophobic pocket is also shown, which is occupied only in the closed conformation (by F292 which is shown in the wild type structure along with L295). For the closed conformation the β6-α7 mainchain trace is broken between F292 and L295 for clarity. On the otherwise grey GRASP surface, hydrophobic residues are colored yellow. (C) The C-terminal fragments encompassing the β6-α7 loop for the three unligated α_L conformations and open and closed α_2 and α_M I domain structures (see color keys). The sidechain bonds of Cys-287 and Cys-294 in the designed disulfide bridge in the high affinity mutant are shown in yellow; the Cα atom of Cys-299 in the designed disulfide of the intermediate mutant is shown as a green sphere.

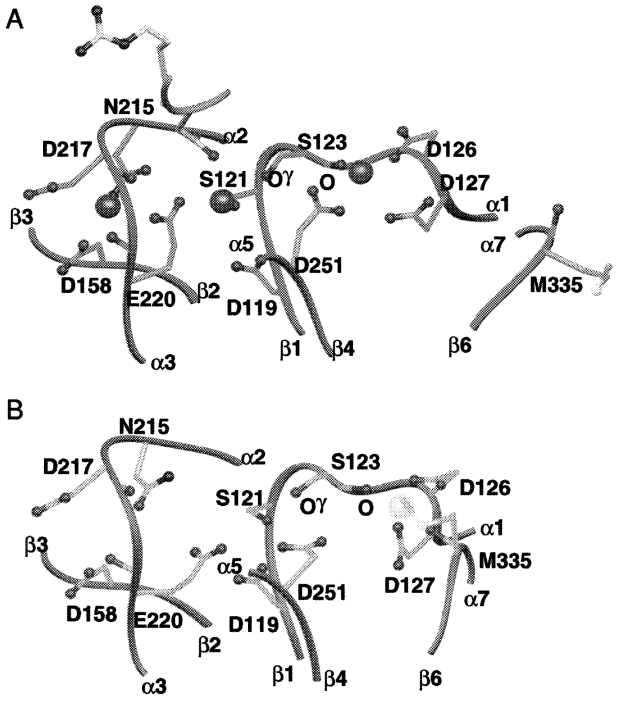

SPRINGER AND WANG, FIG. 7. The linear cluster of metal binding sites in the β I-like domain. (A) The liganded $\alpha_v\beta_3$ structure in Mn^{2+} with RGD (Xiong *et al.*, 2002) in gold. (B) The unliganded $\alpha_v\beta_3$ structure in Ca^{2+} (Xiong *et al.*, 2001). The structures were superimposed by using the I-like domain, so that equivalent positions in (A) and (B) are vertically aligned. The orientation is with the LIMBS, MIDAS, and ADMIDAS from left to right. Mn^{2+} and Ca^{2+} ions are large magenta and yellow spheres, respectively. All putative metal coordinating sidechains and backbone carbonyl groups are shown, with N, O, and S atoms in blue, red, and yellow, respectively. The carbonyl and sidechain oxygens of S123 are marked O and Oγ, respectively.

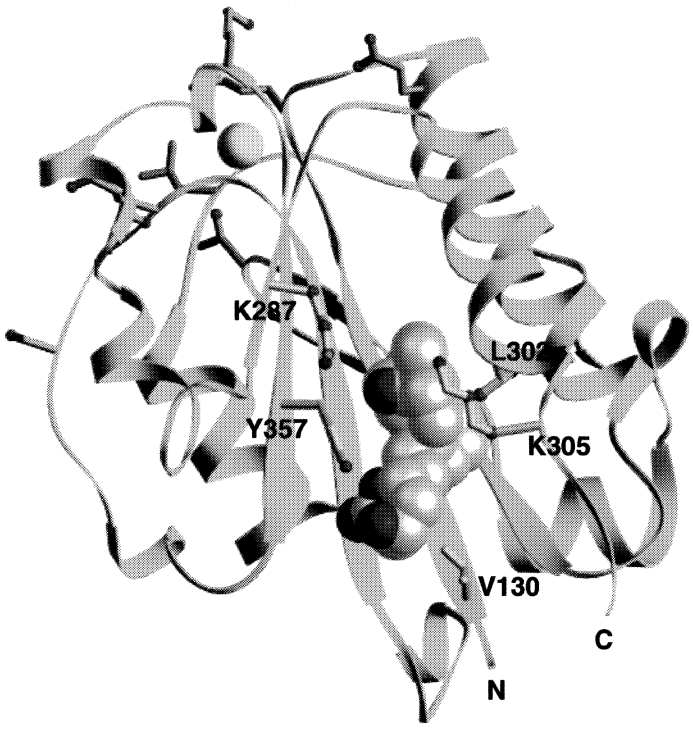

SPRINGER AND WANG, FIG. 8. Ribbon diagram of the α_L I domain in complex with an α I allosteric antagonist (Kallen *et al.*, 1999). The α I allosteric antagonist (shown by CPK with silver carbon atoms and red oxygen atoms) binds in the hydrophobic pocket underneath the C-terminal α-helix and stabilizes the I domain in the closed conformation. The side chains within the antagonist-binding pocket are shown with gold bonds and carbon atoms, red oxygen atoms, and blue nitrogen atoms. The residues critical for binding to ICAM-1 and ICAM-2 are shown with purple side chains and yellow sulfur, red oxygen, and blue nitrogen atoms. Note that these residues are located around the MIDAS, distal from the antagonist binding site.

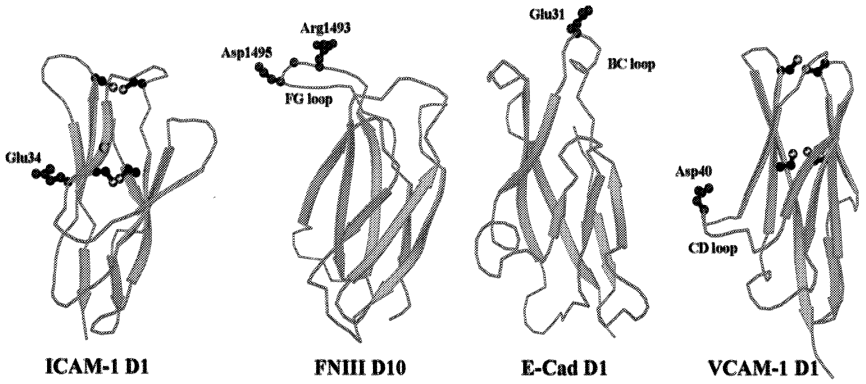

SPRINGER AND WANG, FIG. 9. Ribbon diagram of integrin-binding domain structures of four representative integrin ligands: ICAM-1 domain 1 (ICAM-1 D1), 10th fibronectin type III repeat (FNIII D10), E-cadherin domain 1 (E-Cad D1), and VCAM-1 domain 1 (VCAM-1 D1). In the figure, those key integrin-binding acidic residues are shown in red ball-and-stick model. They are located at the end of the C strand of IgSF domain (ICAM-1 D1), at the tip of the FG loop of FNIII domain (FNIII D10), at the tip of the BC loop of cadherin domain (E-Cad D1), and at the tip of the CD loop of IgSF domain (VCAM-1 D1), respectively. The figure demonstrates the diversity of integrin-binding modes to structurally very similar domains. The figure was prepared with MOLSCRIPT.

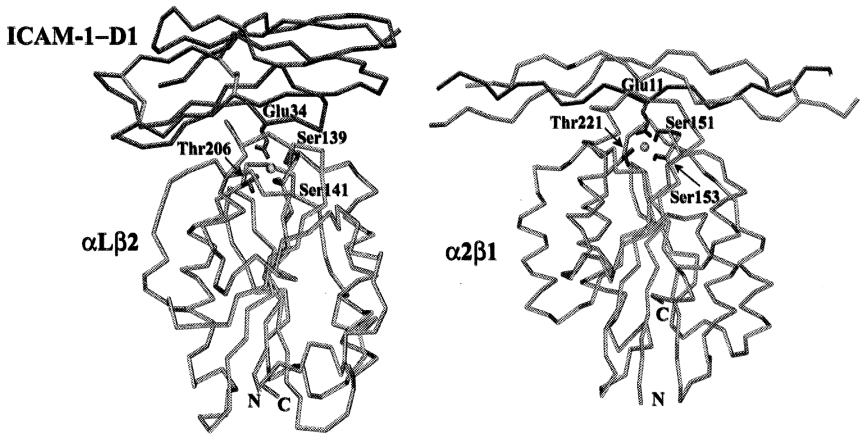

SPRINGER AND WANG, FIG. 10. Backbone diagram of two integrin/ligand complex structures. On the left panel is an intermediate affinity I domain from $\alpha_L\beta_2$ (in blue) in complex with ICAM-1 (in red). For clarity, only ICAM-1 D1 is shown. The sidechains of the key integrin-binding residue, Glu34, of ICAM-1 and MIDAS residues that directly coordinate the metal (in yellow) are illustrated. On the right panel is an I domain from $\alpha_2\beta_1$ (in blue) in complex with synthetic collagen-originated 21-mer triple-peptides (the major interacting middle strand is in red, and the other two strands are in yellow and green, respectively). Also, sidechains of the key integrin-binding residue, Glu11, of collagen and MIDAS residues of I domain are illustrated. The figure was prepared with SETOR.